RECENT EXPERIMENTAL RESULTS FROM AUSTRALIA INVESTIGATING QUASIFISSION DYNAMICS

D.J. Hinde, M. Dasgupta, D.Y. Jeung, C. Simenel, E.C. Simpson, B.M.A. Swinton-Bland, E. Prasad, E. Williams, K. Banerjee, I.P Carter, K.J. Cook, S. Kalkal, D. Rafferty, C. Sengupta, K. Vo Phuoc, J. Walshe

Department of Nuclear Physics, Research School of Physics and Engineering

Australian National University, Canberra, ACT 2601, Australia

H.M. David[1], Ch. E. Düllmann[1,2,3], J. Khuyagbaatar[1,2], A Yakushev[1,2]

1) GSI/FAIR Darmstadt

2) Helmholtz Institut Mainz, Germany

3) University of Mainz, Germany

$$P_{SHE} = P_{capture} \cdot P_{CN} \cdot W_{fission\ survival}(E, L)$$

QUASIFISSION ⟶ $P_{CN} << 1$

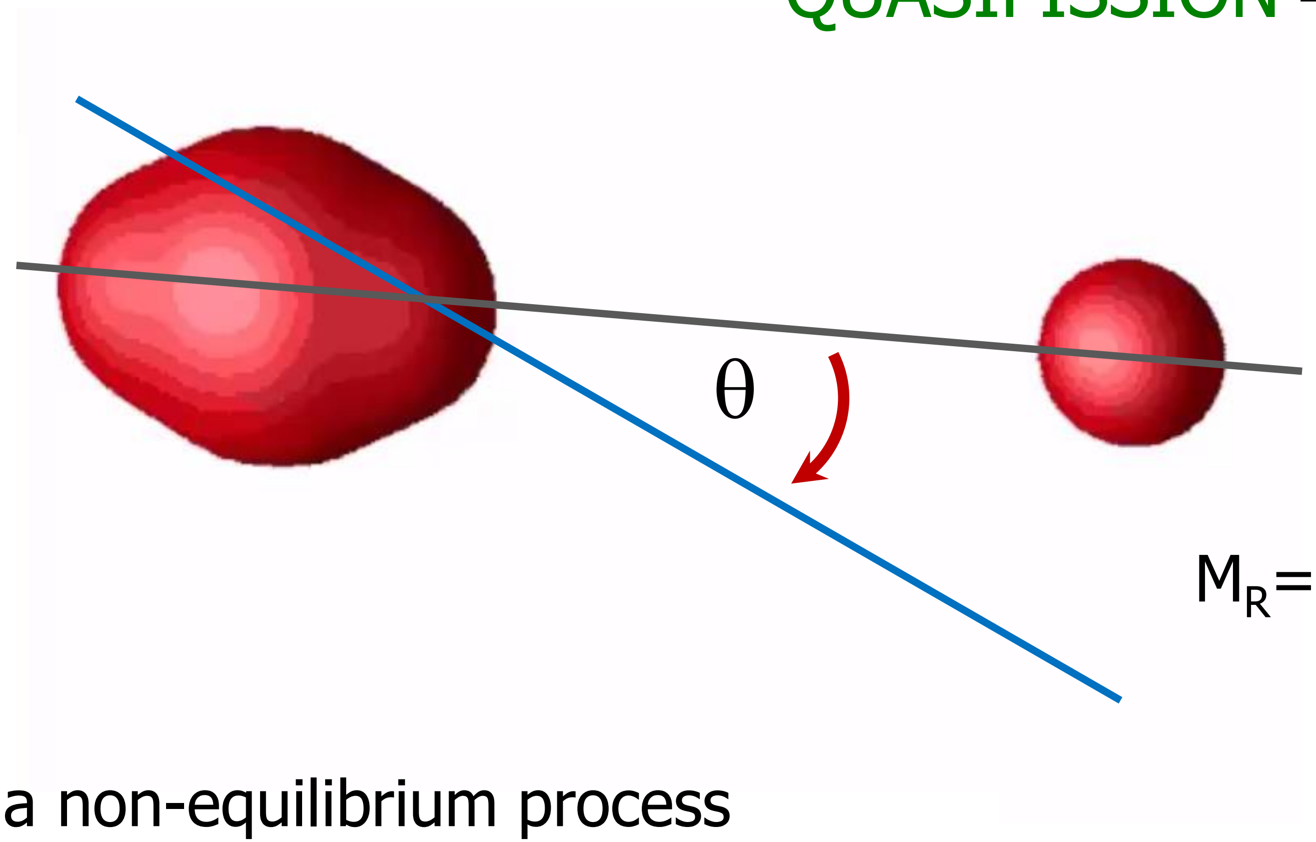

b > 0

$M_R = M_1/(M_1+M_2)$

TDHF: $^{40}Ca + ^{238}U$

A. Wakhle, C. Simenel et al.

PRL **113** (2014) 182502

Quasifission a non-equilibrium process

Time-scale is a key characteristic ($zs = 10^{-21}s$)

ANU experiments

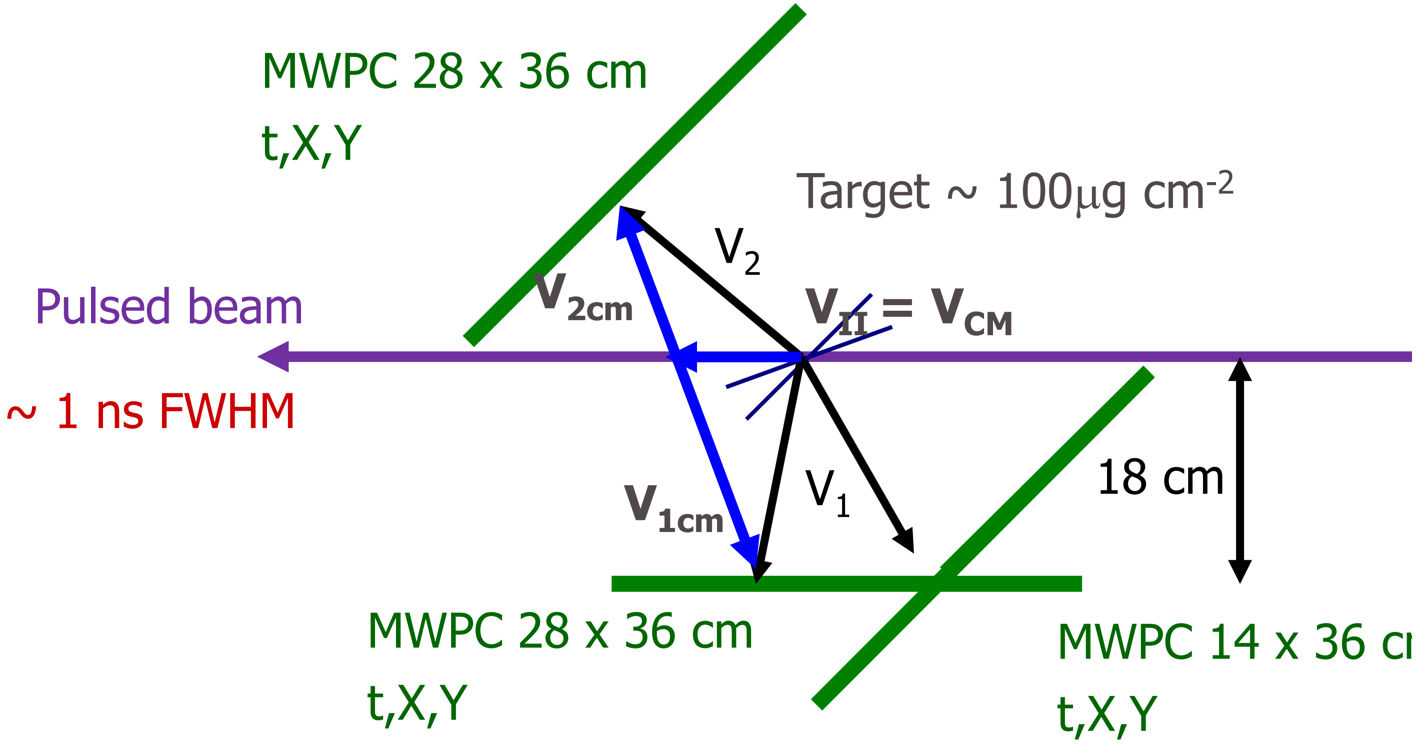

Kinematic coincidence:

Hinde et al., PRC **53** (1996) 1290
Rafiei et al., PRC **77** (2008) 024606
Thomas et al., PRC **77** (2008) 034610
Hinde et al., PRL **100** (2008) 202701
Hinde et al., PRL **101** (2008) 092701
du Rietz et al., PRL **106** (2011) 052701

Lin et al., PRC **85** (2012) 014611
Simenel et al., PLB 710 (2012) 607
Williams et al., PRC **88** (2013) 034611
du Rietz et al., PRC **88** (2013) 054618
Wakhle et al., PRL **113** (2014) 182502
Hammerton et al., PRC **91** (2015)041602

Prasad et al., PRC **91** (2015)064605
Khuyagbaatar et al., PRC **91** (2015) 054608
Prasad et al., PRC **93** (2016) 024608
Prasad et al., PRC **96** (2017) 034608
Morjean et al., PRL **119** (2017) 222512
Williams et al., PRL **120** (2018) 022501

Hinde et al., PRC **97** (2018) 024616
Wakhle et al., PRC **97** (2018) 021602
Mohanto et al., PRC **97** (2018) 054603
Khuyagbaatar et al., PRC **97** (2018) 064618
K. Banerjee et al., 2019 under review
H. David et al., 2019 under review

MAD – time scales of mass-equilibration and rotation (GSI)

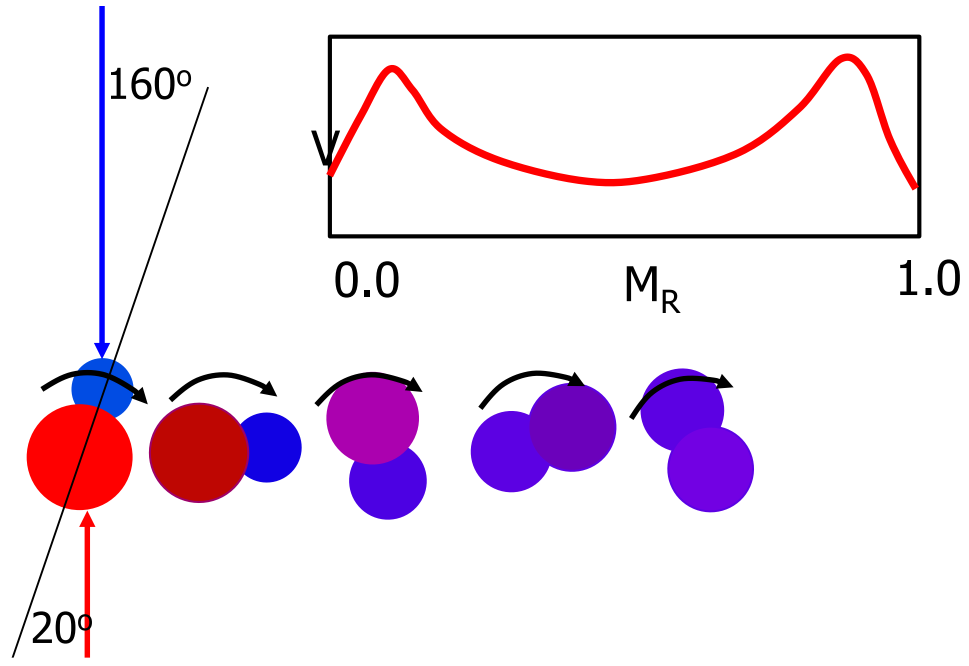

R. Bock et al., NP **A388** (1982) 334

J. Toke et al., NP **A440** (1985) 327

W.Q. Shen at al., PRC **36** (1987) 115

B.B. Back et al., PRC **53** (1996) 1734

Mass-angle distributions – MAD

R. Bock et al., NP **A388** (1982) 334
J. Toke et al., NP **A440** (1985) 327
W.Q. Shen at al., PRC **36** (1987) 115
B.B. Back et al., PRC **53** (1996) 1734

GSI

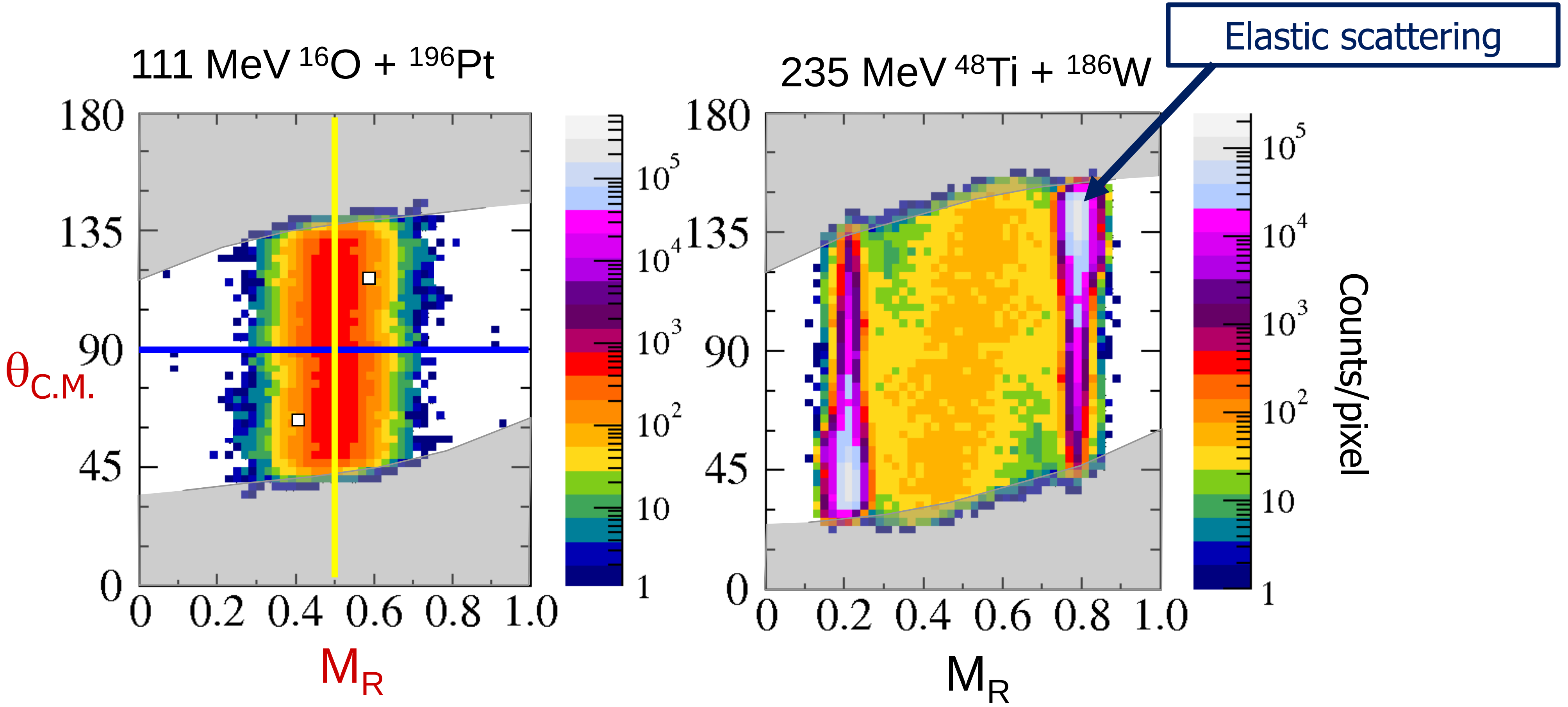

"Magic" reactions with ^{208}Pb – "cold fusion"

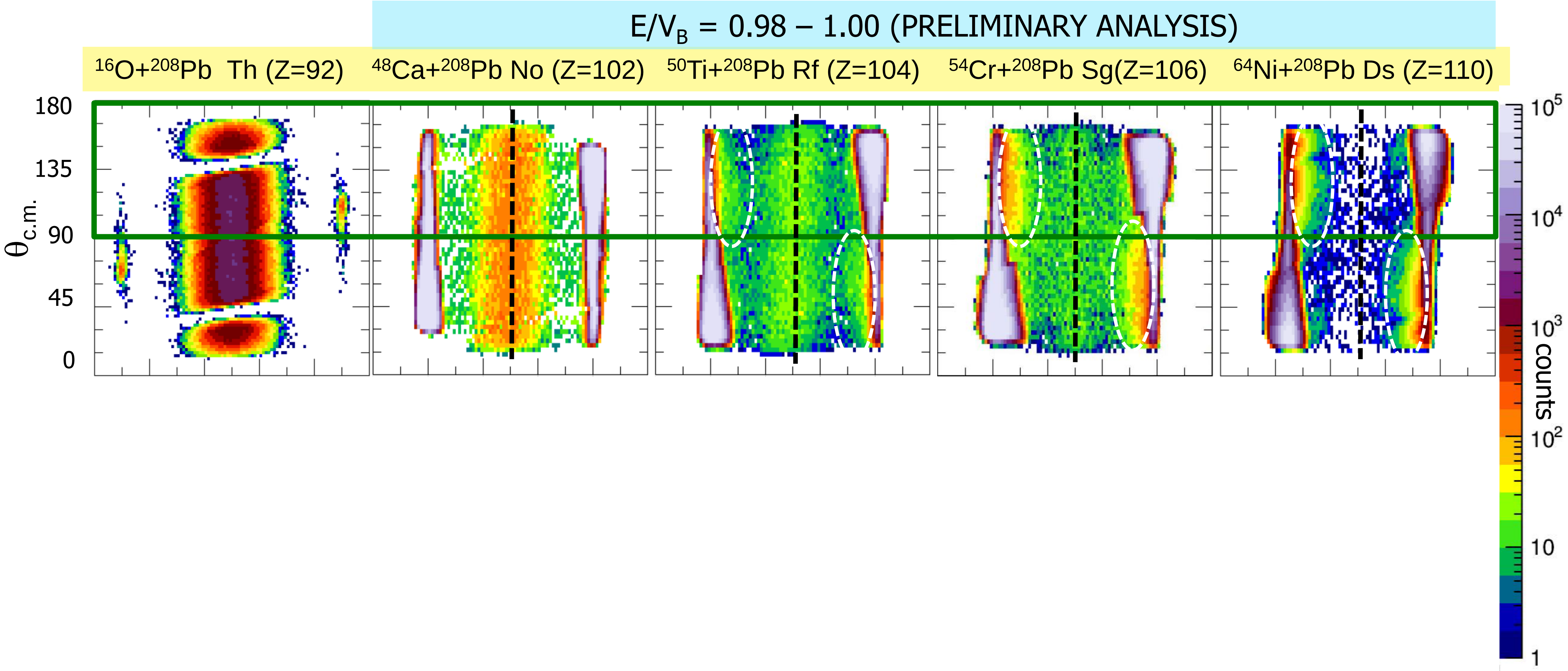

Effects of nuclear structure in the entrance channel:
(i) Spherical magic nuclei and N/Z matching in cold fusion

^{258}Sg	^{258}Sg	^{258}Sg
$^{54}_{24}Cr_{30}$ + $^{204}_{82}Pb_{122}$	$^{50}_{24}Cr_{26}$ + $^{208}_{82}Pb_{126}$	$^{52}_{24}Cr_{28}$ + $^{206}_{82}Pb_{124}$

(Z=106) ^{258}Sg

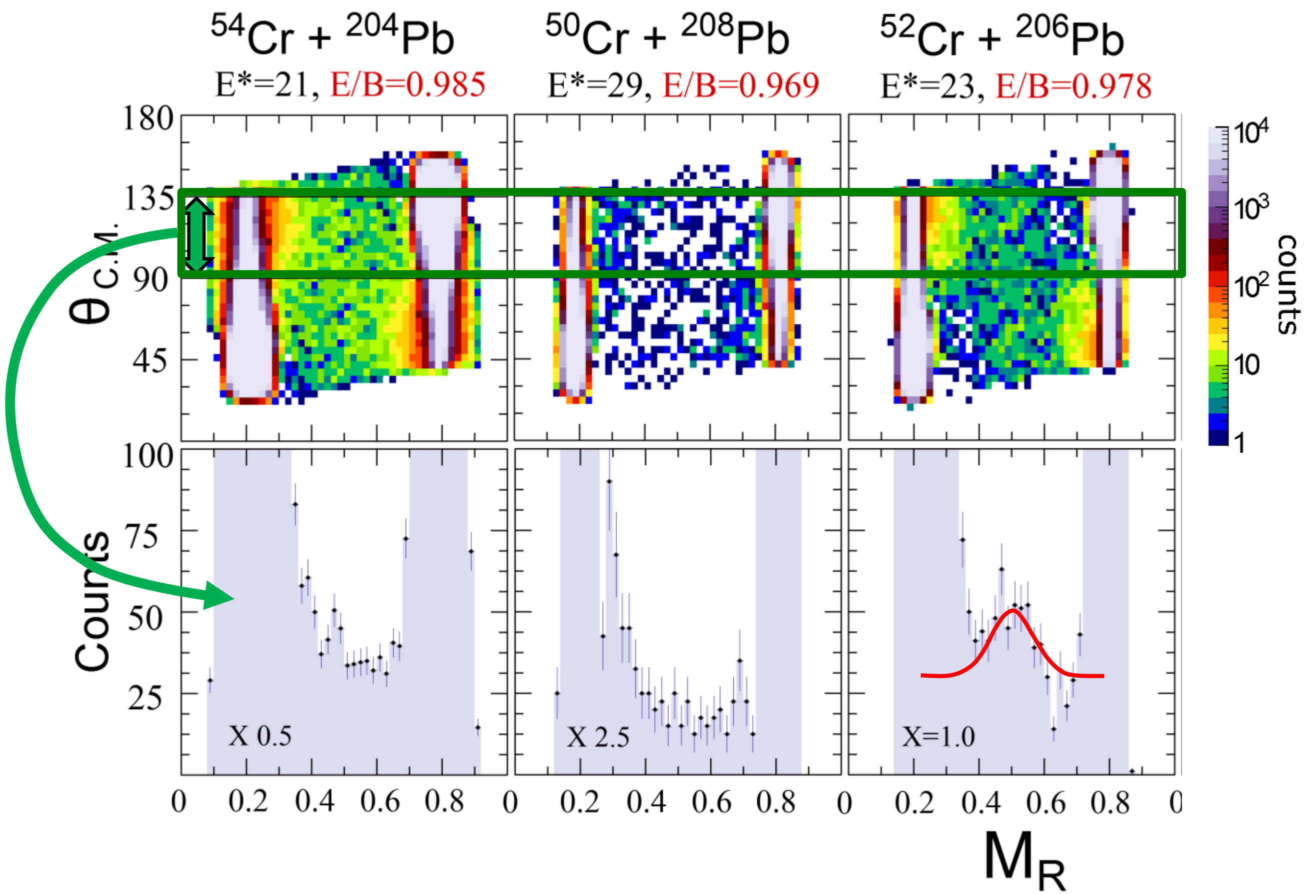

Xeff = 0.763
$N_M = 1$
$\Delta_{(N/Z)} = 0.24$

Xeff = 0.782
$N_M = 2$
$\Delta_{(N/Z)} = 0.45$

Xeff = 0.772
$N_M = 2$
$\Delta_{(N/Z)} = 0.35$

G. Mohanto et al., PRC97(2018)054603

Energy below barrier: magic numbers, N/Z matching – strong effect

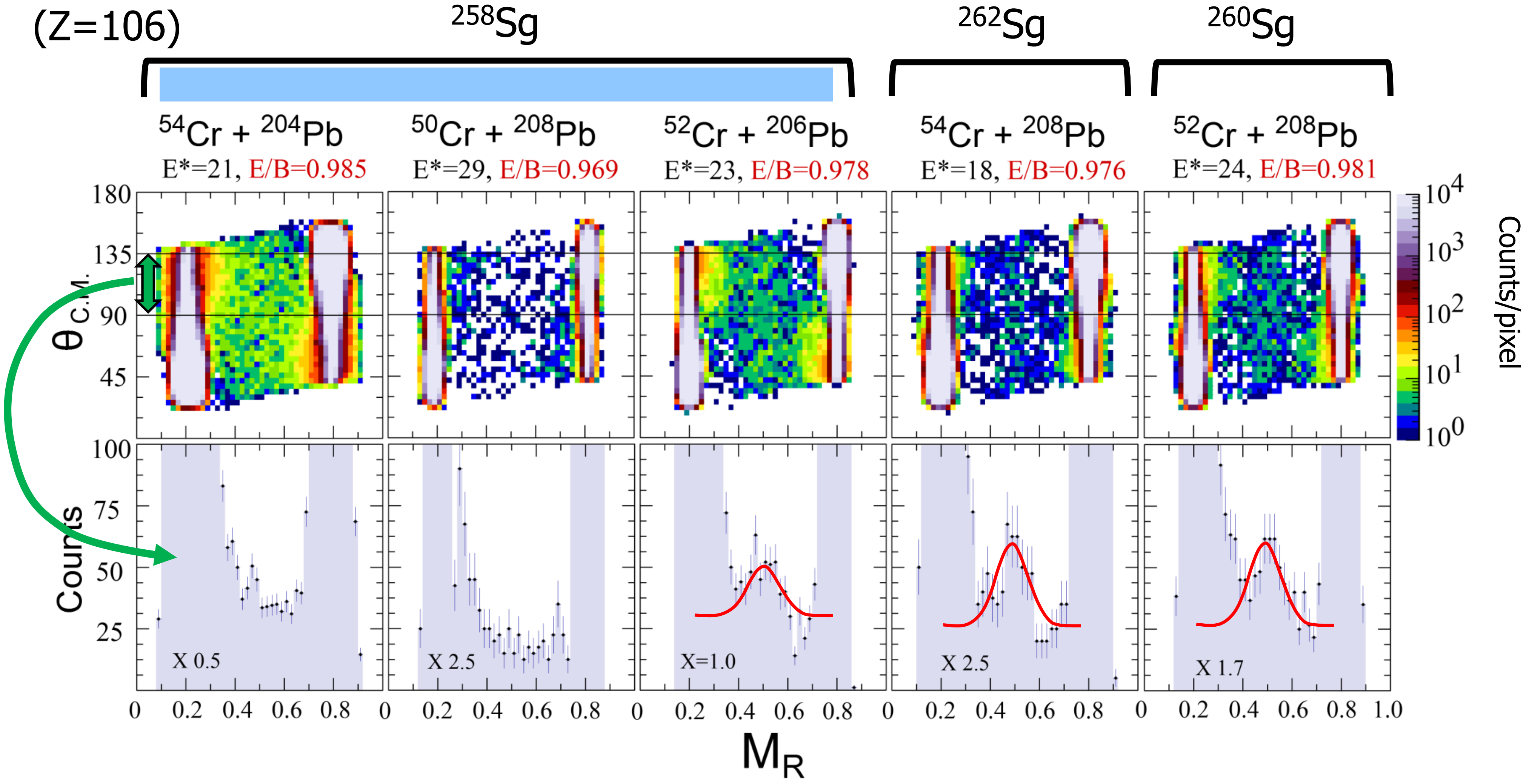

Xeff = 0.763	Xeff = 0.782	Xeff = 0.772	Xeff = 0.761	Xeff = 0.771
$N_M = 1$	$N_M = 2$	$N_M = 2$	$N_M = 2$	$N_M = 3$
$\Delta_{(N/Z)} = 0.24$	$\Delta_{(N/Z)} = 0.45$	$\Delta_{(N/Z)} = 0.35$	$\Delta_{(N/Z)} = 0.29$	$\Delta_{(N/Z)} = 0.37$

G. Mohanto et al., PRC97(2018)054603

Energy below barrier: magic numbers, N/Z matching – strong effect

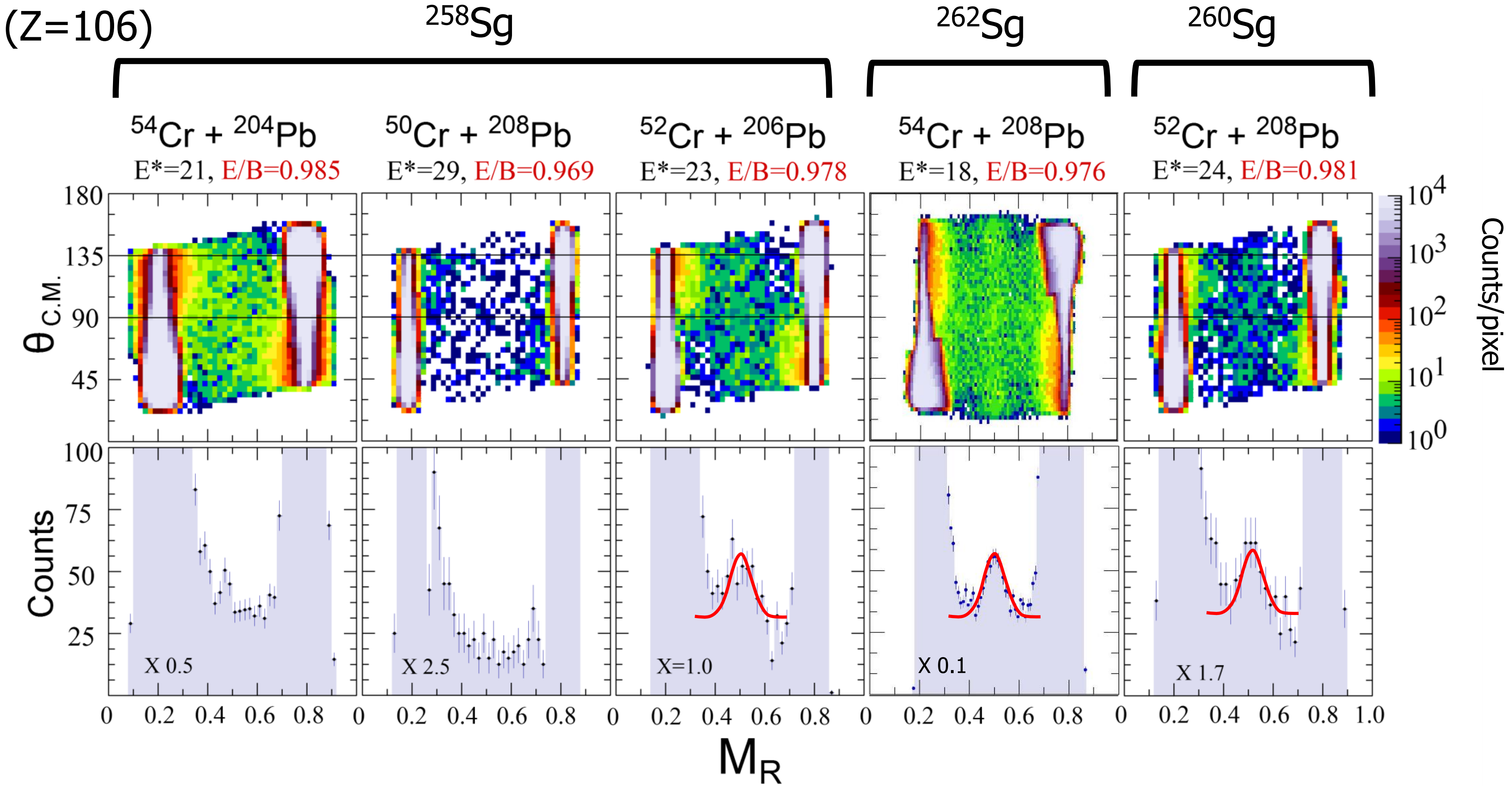

Xeff = 0.763	Xeff = 0.782	Xeff = 0.772	Xeff = 0.761	Xeff = 0.771
$N_M = 1$	$N_M = 2$	$N_M = 2$	$N_M = 2$	$N_M = 3$
$\Delta_{(N/Z)} = 0.24$	$\Delta_{(N/Z)} = 0.45$	$\Delta_{(N/Z)} = 0.35$	$\Delta_{(N/Z)} = 0.29$	$\Delta_{(N/Z)} = 0.37$

G. Mohanto et al., PRC97(2018)054603

Energy well above-barrier: magic numbers, N/Z matching – smaller effect

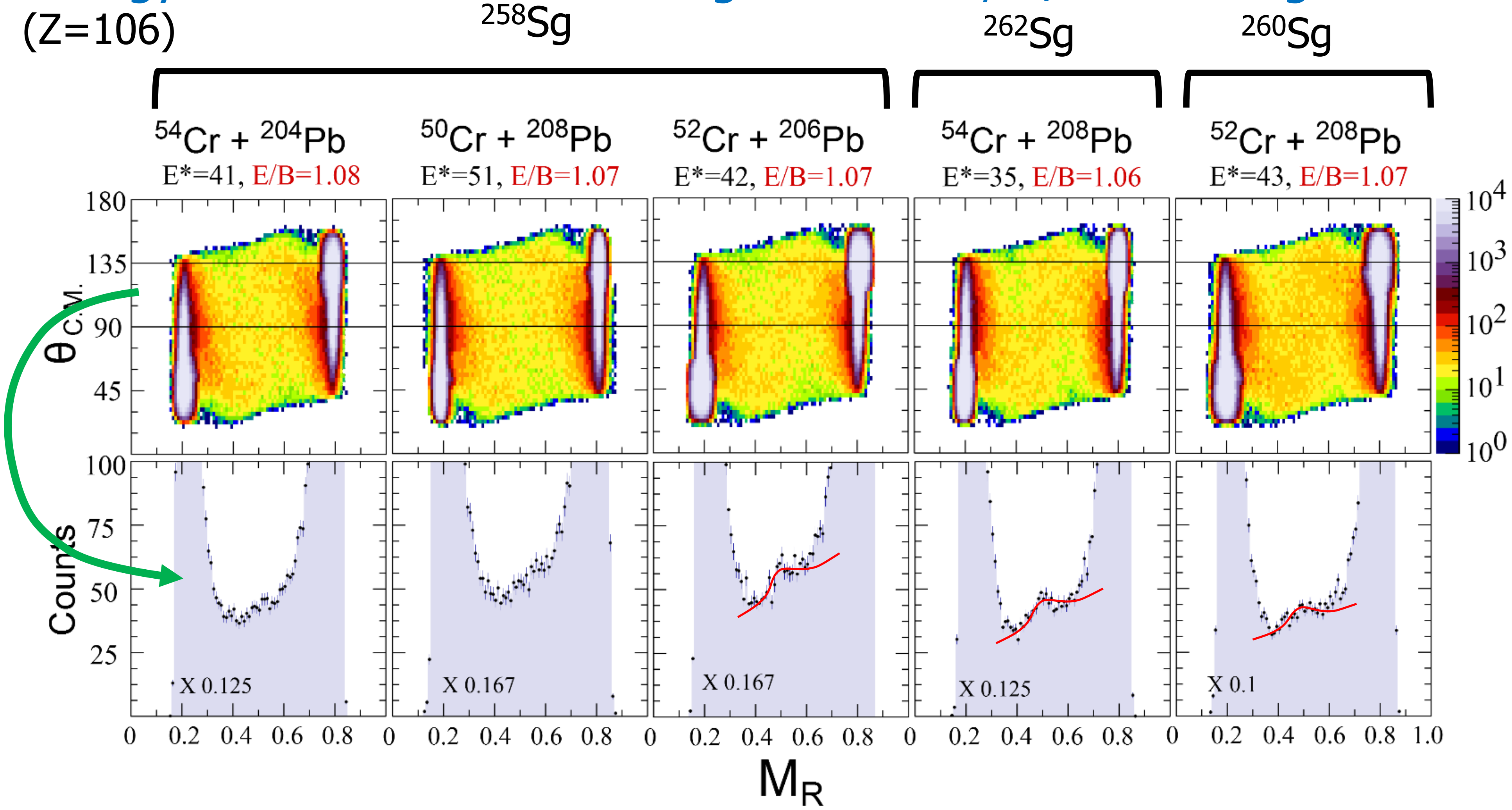

Xeff = 0.763, N_M = 1, $\Delta_{(N/Z)}$ = 0.24

Xeff = 0.782, N_M = 2, $\Delta_{(N/Z)}$ = 0.45

Xeff = 0.772, N_M = 2, $\Delta_{(N/Z)}$ = 0.35

Xeff = 0.761, N_M = 2, $\Delta_{(N/Z)}$ = 0.29

Xeff = 0.771, N_M = 3, $\Delta_{(N/Z)}$ = 0.37

G. Mohanto et al., ANU, in preparation

Conclusions

- Magic numbers, N/Z matching important in cold fusion reactions

    magic numbers, N/Z matching: – $^{48}Ca+^{208}Pb$ – exceptional!

    trajectory bifurcation $^{52,54}Cr + ^{206,208}Pb$ – fast QF + F-F

"HOT" FUSION reactions with prolate deformed actinide target nuclei

ANU: Th, U targets; Mainz/GSI: Pu, Cm, Cf targets

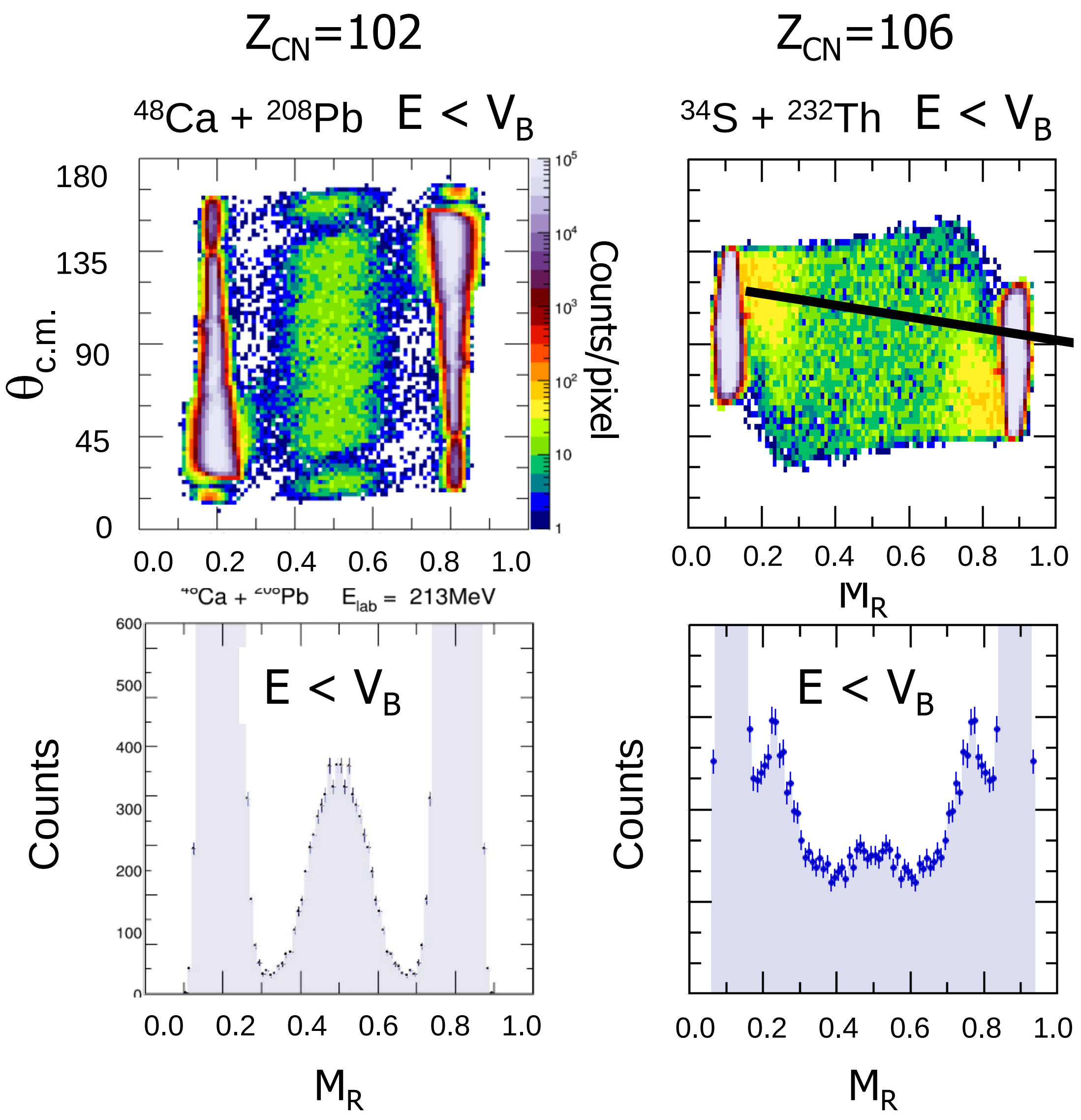

Effects of nuclear structure in the entrance channel:
(ii) Static deformation alignment in “hot fusion”. Low E_X = “tip” collisions

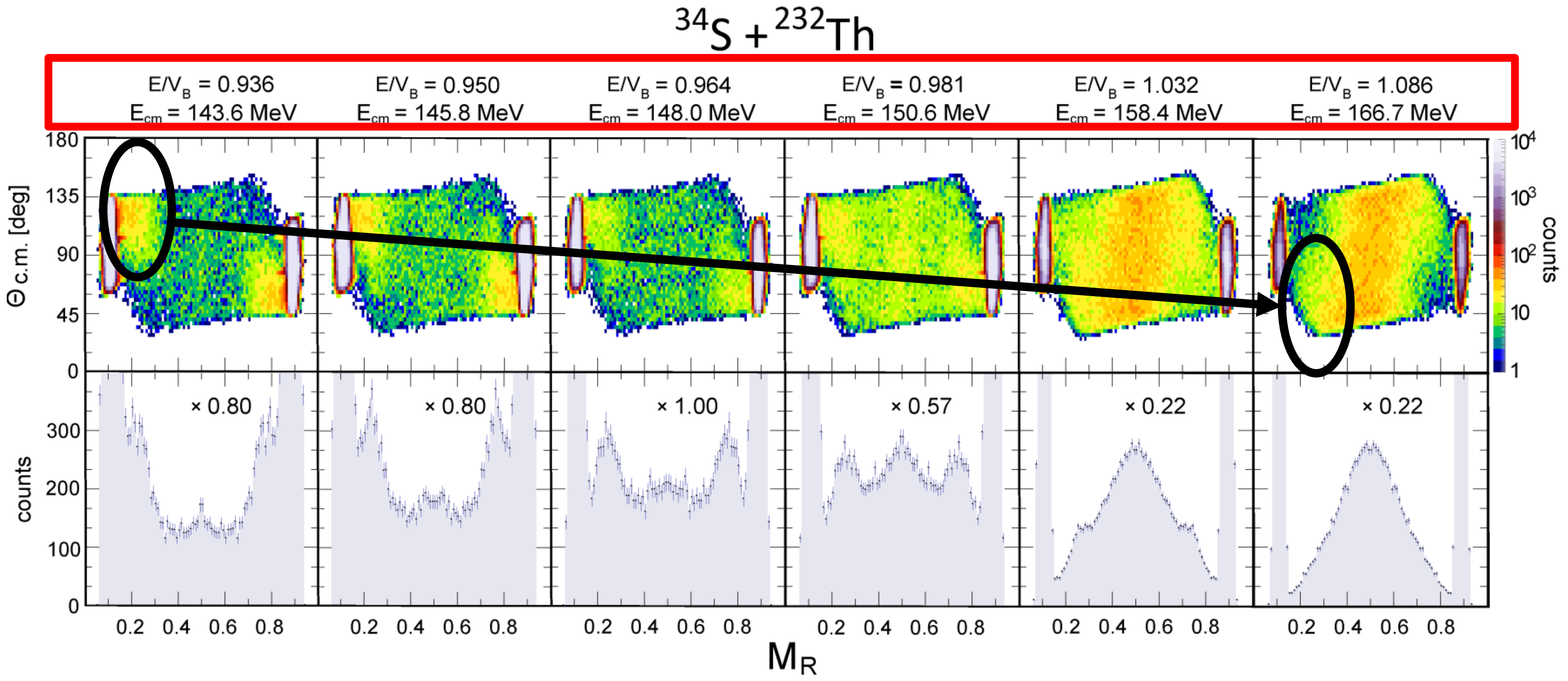

$^{34}S + ^{232}Th \rightarrow ^{266}Sg$

(Z=106)

Deformation aligned (axial or tip) collisions

Effects of nuclear structure in the entrance channel:

(ii) Static deformation alignment in "hot fusion". Low E_X = "tip" collisions

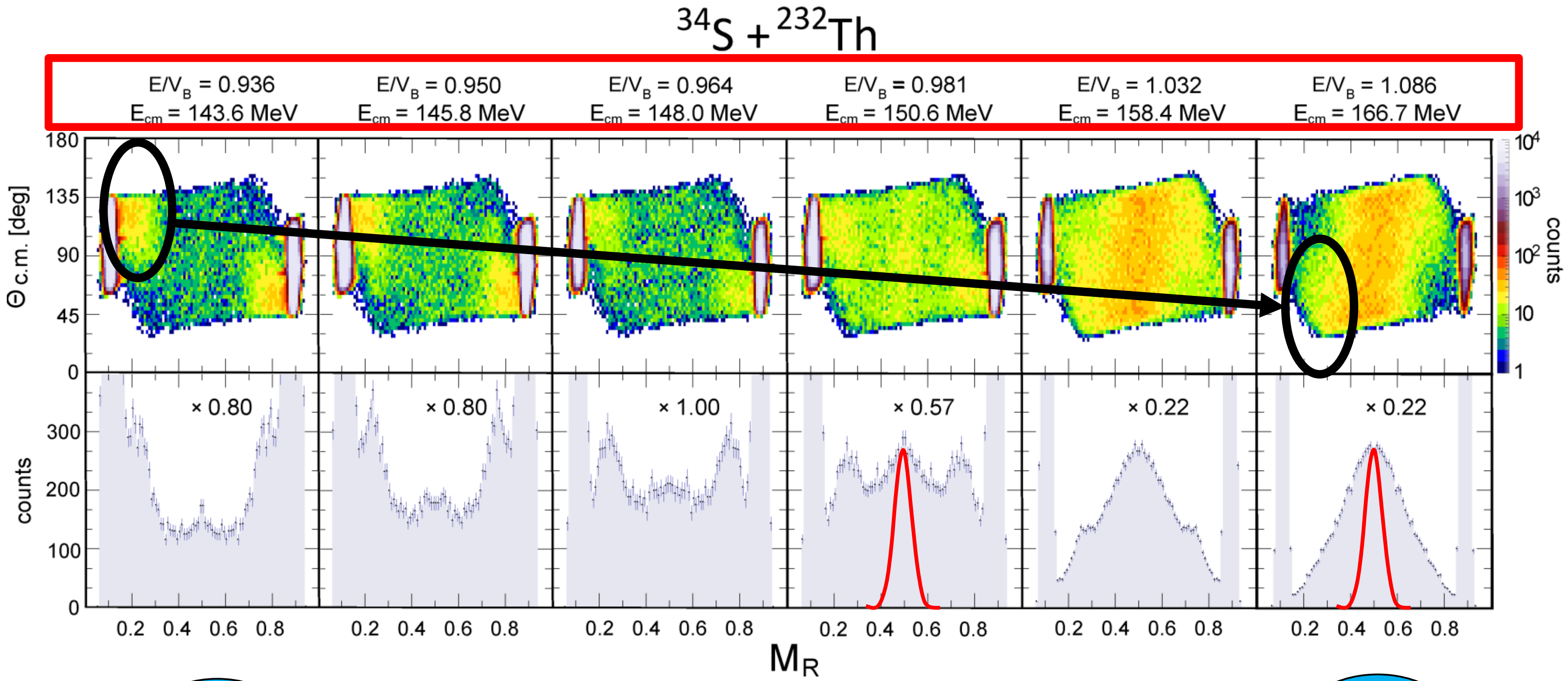

$^{34}S + ^{232}Th \rightarrow ^{266}Sg$

(Z=106)

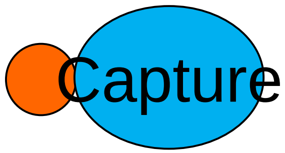

Deformation aligned (axial or tip) collisions

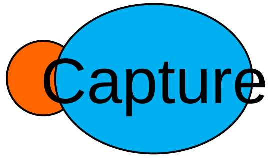

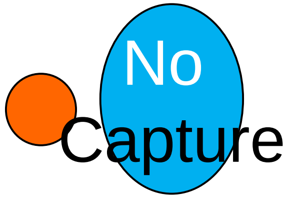

Equatorial or side collisions

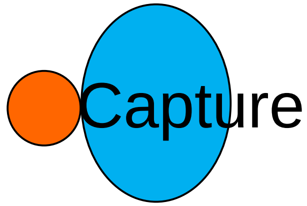

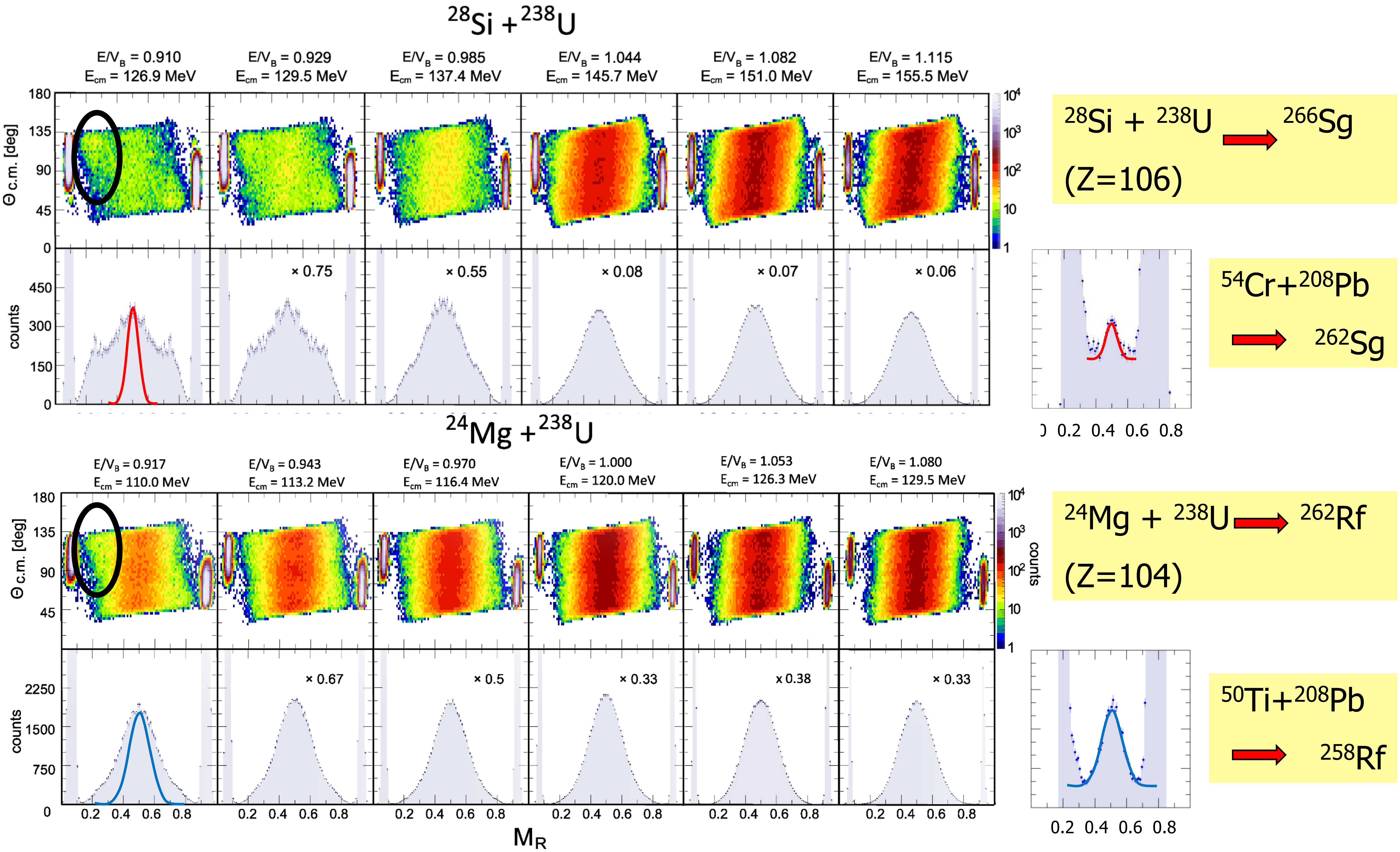

$^{28}Si + ^{238}U$
E/V_B = 0.910 E_cm = 126.9 MeV
E/V_B = 0.929 E_cm = 129.5 MeV
E/V_B = 0.985 E_cm = 137.4 MeV
E/V_B = 1.044 E_cm = 145.7 MeV
E/V_B = 1.082 E_cm = 151.0 MeV
E/V_B = 1.115 E_cm = 155.5 MeV
× 0.75
× 0.55
× 0.08
× 0.07
× 0.06
$^{24}Mg + ^{238}U$
E/V_B = 0.917 E_cm = 110.0 MeV
E/V_B = 0.943 E_cm = 113.2 MeV
E/V_B = 0.970 E_cm = 116.4 MeV
E/V_B = 1.000 E_cm = 120.0 MeV
E/V_B = 1.053 E_cm = 126.3 MeV
E/V_B = 1.080 E_cm = 129.5 MeV
× 0.67
× 0.5
× 0.33
× 0.38
× 0.33
Θ c.m. [deg]
counts
M_R
$^{28}Si + ^{238}U \rightarrow ^{266}Sg$ (Z=106)
$^{54}Cr + ^{208}Pb \rightarrow ^{262}Sg$
$^{24}Mg + ^{238}U \rightarrow ^{262}Rf$ (Z=104)
$^{50}Ti + ^{208}Pb \rightarrow ^{258}Rf$

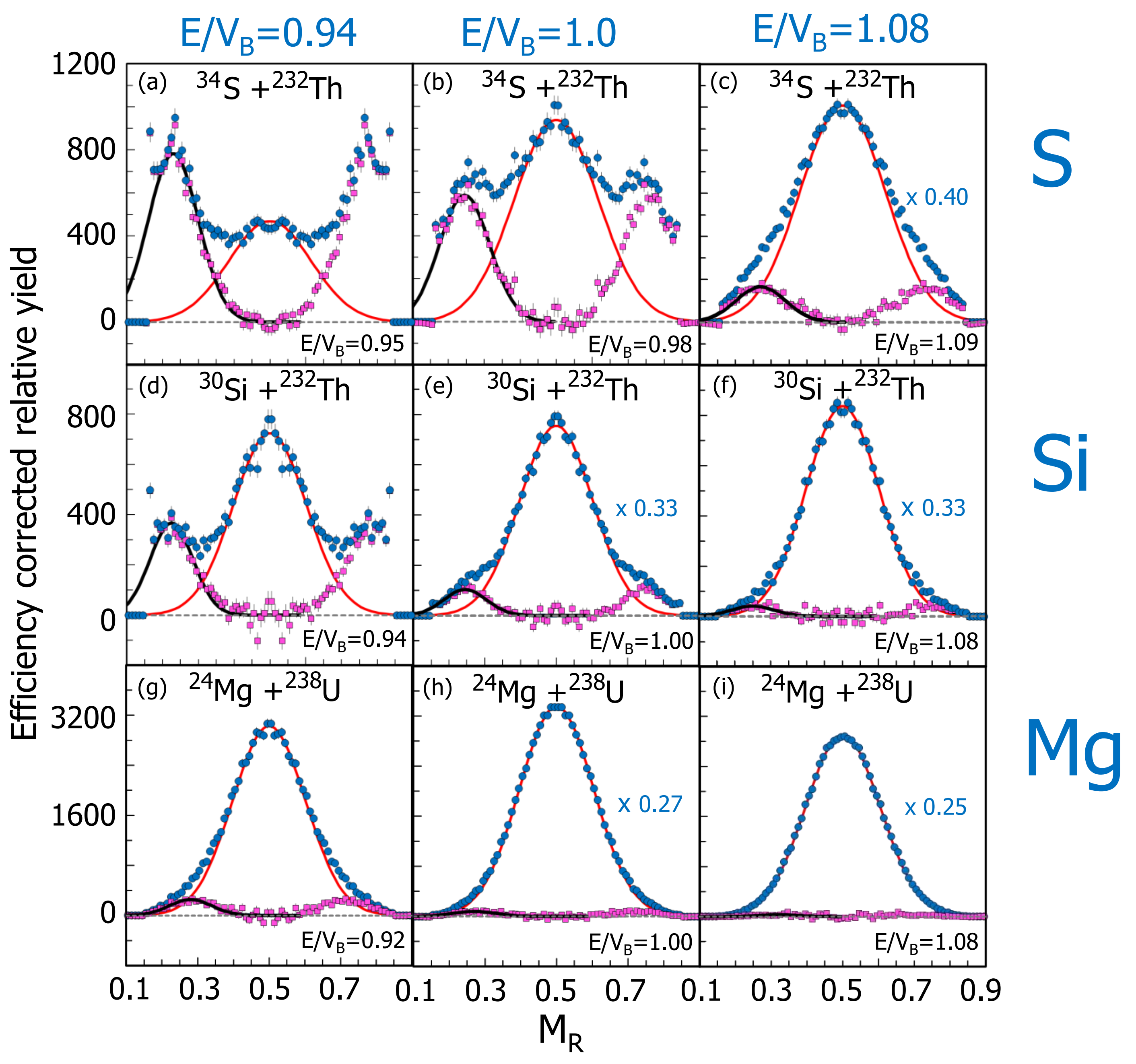

E/V_B=0.94
E/V_B=1.0
E/V_B=1.08
(a) 34S + 232Th
(b) 34S + 232Th
(c) 34S + 232Th
(d) 30Si + 232Th
(e) 30Si + 232Th
(f) 30Si + 232Th
(g) 24Mg + 238U
(h) 24Mg + 238U
(i) 24Mg + 238U
E/V_B=0.95
E/V_B=0.98
E/V_B=1.09
E/V_B=0.94
E/V_B=1.00
E/V_B=1.08
E/V_B=0.92
E/V_B=1.00
E/V_B=1.08
x 0.40
x 0.33
x 0.33
x 0.27
x 0.25
S
Si
Mg
Efficiency corrected relative yield
M_R

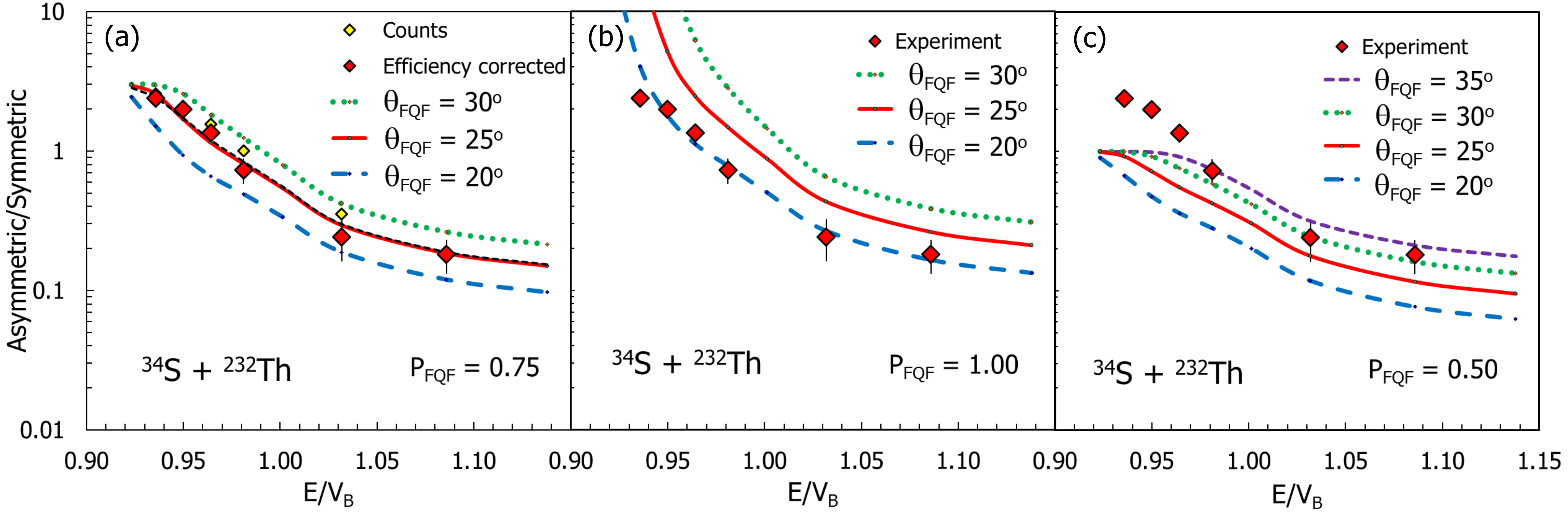

Far below V_B, all capture reactions are in the axial (deformation aligned) configuration

Dependence of tip/side collision σ calculated with CC capture model (CCFULL,CCMOD)

Vary θ_{FQF} and P_{FQF} for tip collisions to reproduce experiment

Hinde et al., PRC **97** (2018) 024616

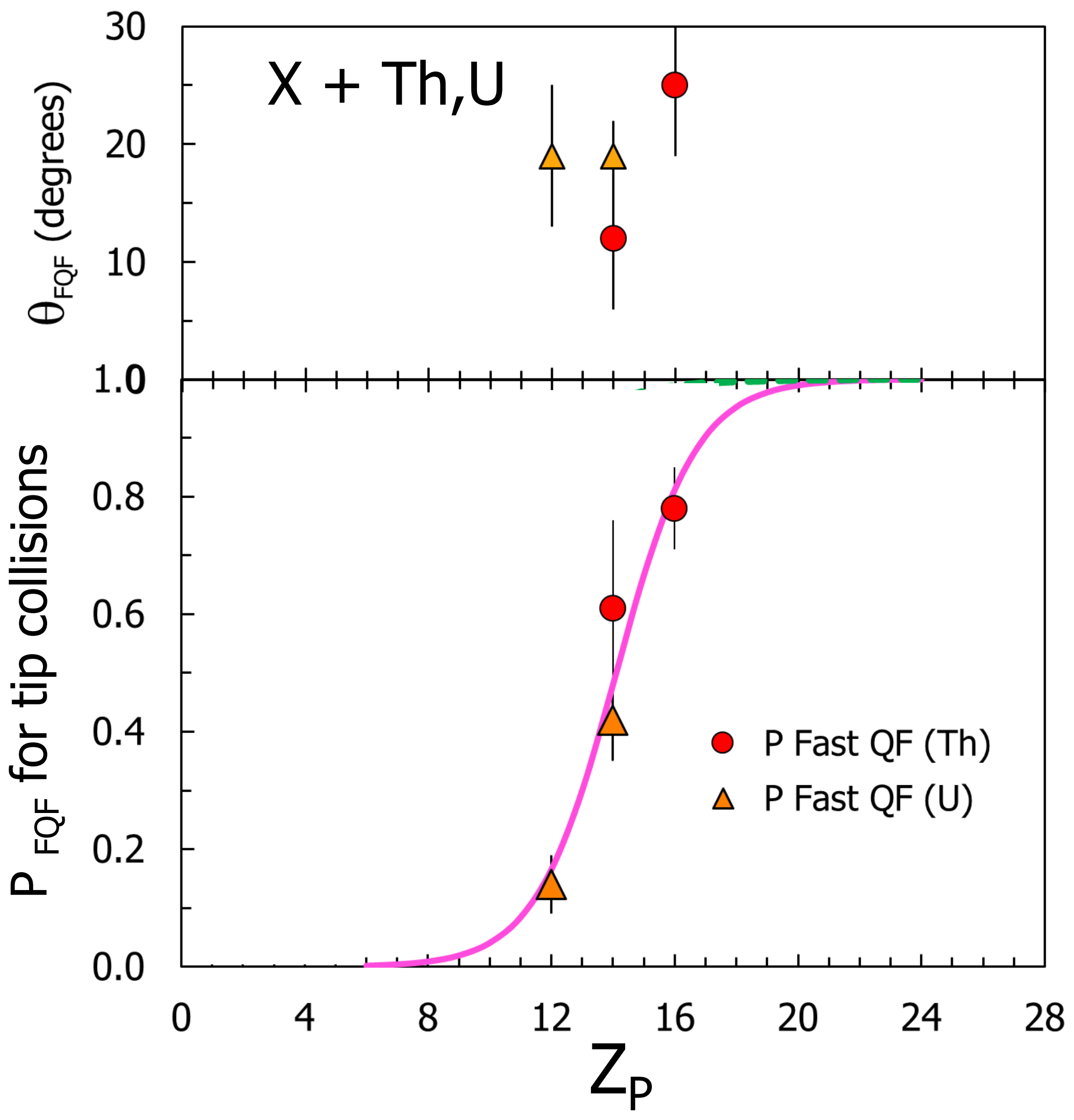

X + Th,U
θ_{FQF} (degrees)
30
20
10
1.0
0.8
0.6
0.4
0.2
0.0
P $_{FQF}$ for tip collisions
P Fast QF (Th)
P Fast QF (U)
0
4
8
12
16
20
24
28
Z_P

Deformation alignment – experiment vs. TDHF $^{40}Ca+^{238}U$

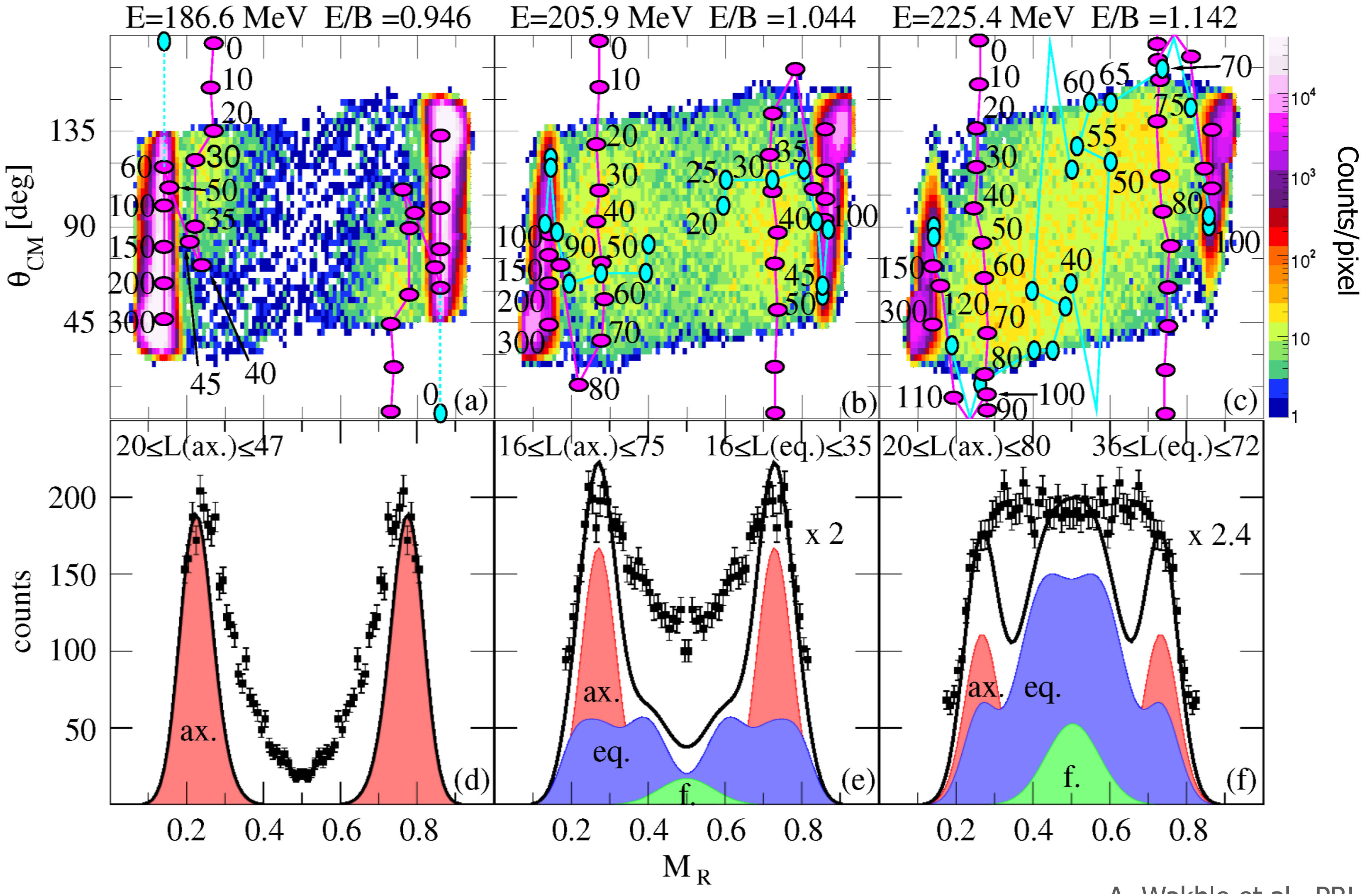

A. Wakhle et al., PRL **113** (2014) 182502

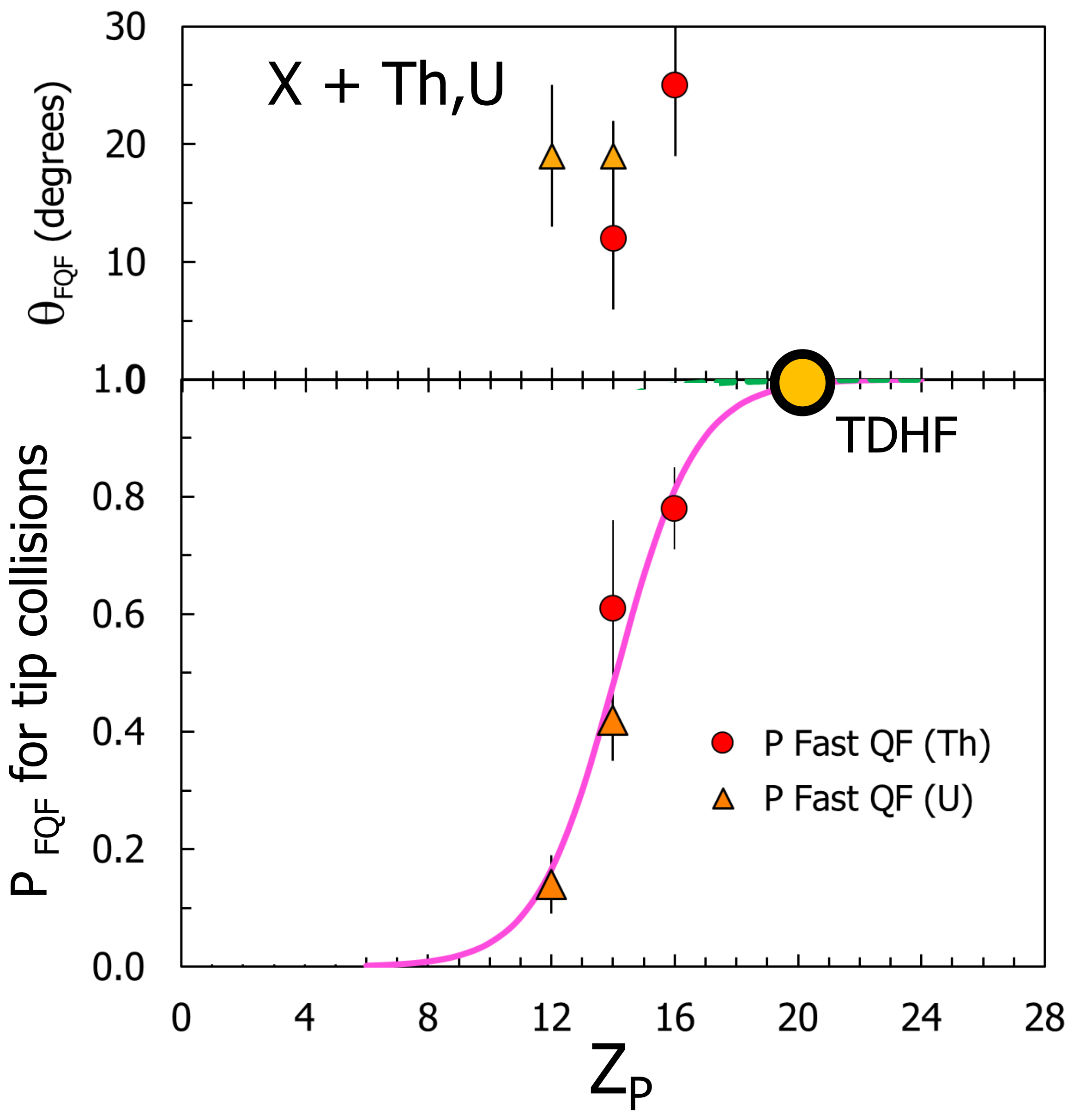

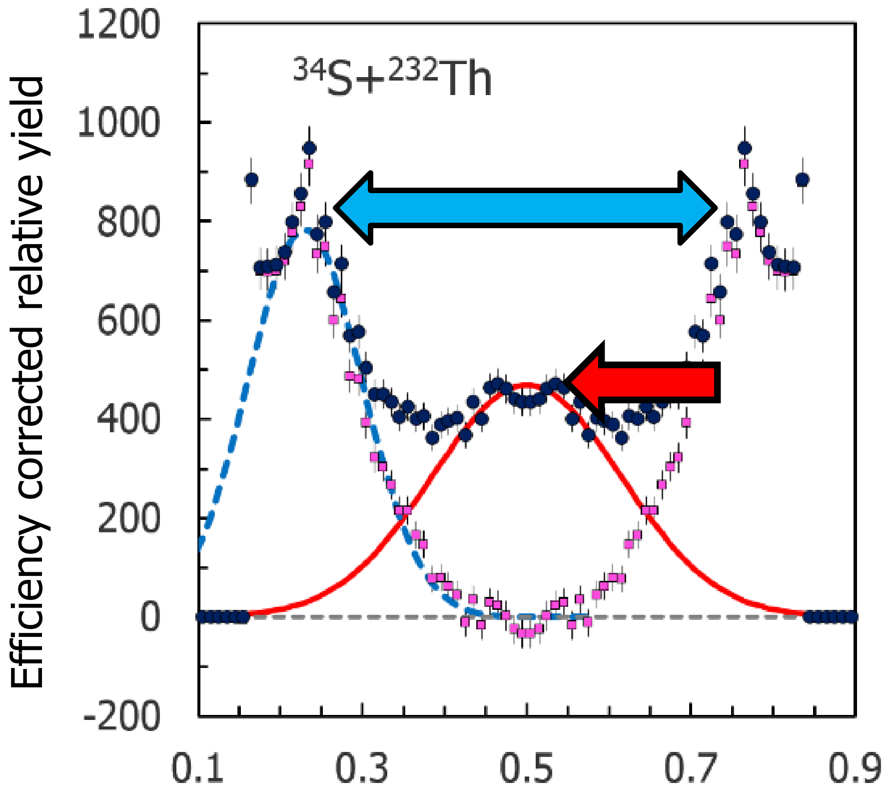

Mass-angle correlation (GSI, ANU)

Mass Distribution (Dubna, JAEA, ANU)

TKE distributions (Dubna)

Angular distributions (....ANU....)

$^{16}O + ^{238}U$

D.J. Hinde et al., PRC **53** (1996) 1290

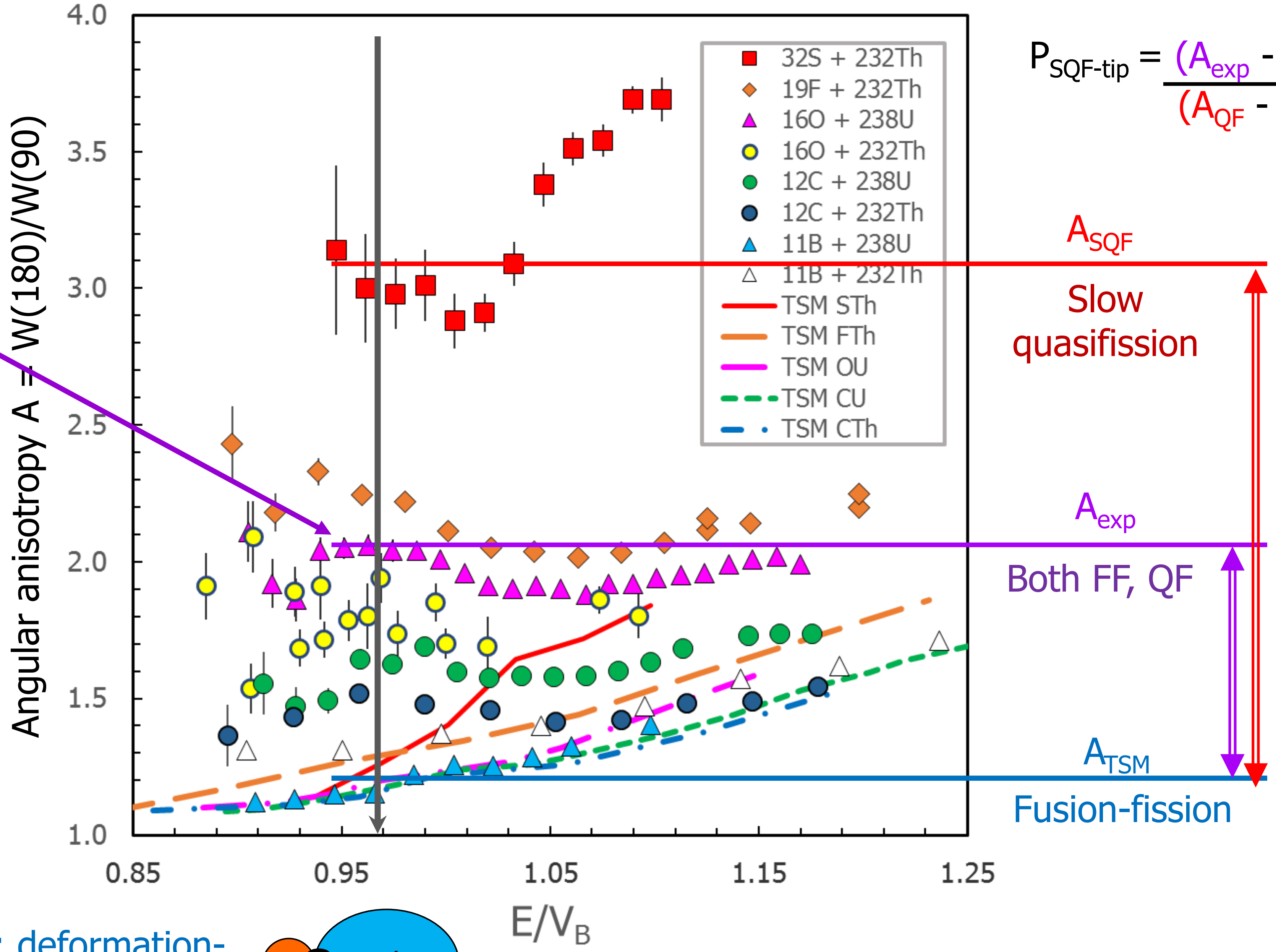

$$P_{SQF\text{-}tip} = \frac{(A_{exp} - A_{TSM})}{(A_{QF} - A_{TSM})}$$

Sub-barrier: deformation-aligned (tip) collisions

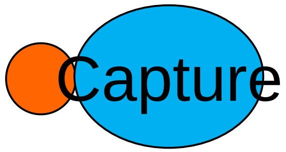

Hinde et al., PRC **97** (2018) 024616

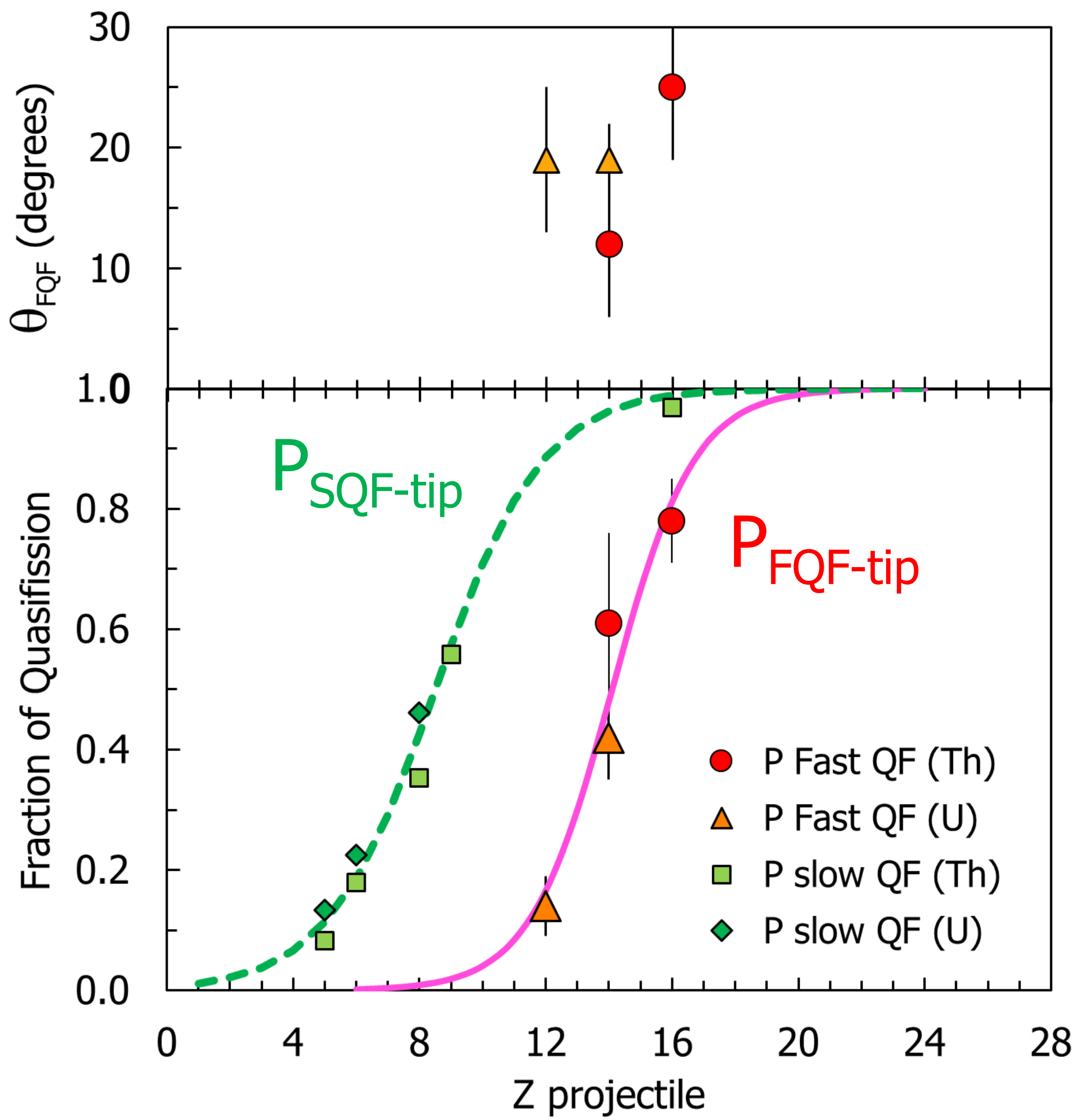

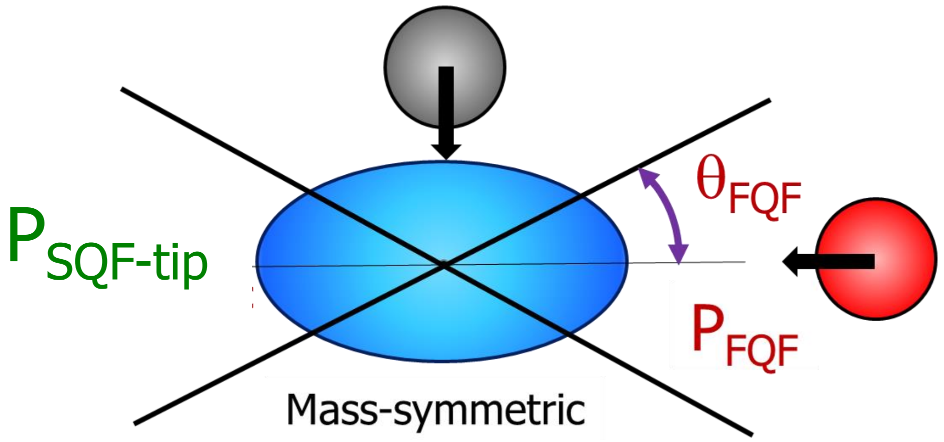

Sub-barrier (axial or tip collisions):

Fast mass-asymmetric QF: P_{FQF}

Slow “mass-symmetric” QF: P_{SQF}

$$P_{CN\text{-}tip} = (1 - P_{FQF})(1 - P_{SQF})$$

Sub-barrier energy, deformed actinide targets:

P_{CN} heavily suppressed by both fast and slow quasifission

Conclusions

- Magic numbers, N/Z matching important in cold fusion reactions

  magic numbers, N/Z matching: – ^{48}Ca+^{208}Pb – exceptional!

  trajectory bifurcation ^{52,54}Cr + ^{206,208}Pb – fast QF + F-F

- Deformation alignment – "tip collisions" – low P_{CN}

  fast QF below-barrier – measured P_{FQF}

  also slow QF below-barrier – P_{SQF} - further reduction of P_{CN}

  (another trajectory bifurcation)

- Challenge for models of SHE synthesis: describe competing processes…

  Effects of nuclear structure in entrance-channel deformation, closed shells, transfer reactions

  Average collision outcomes

  Fluctuations, trajectory bifurcations and probabilities

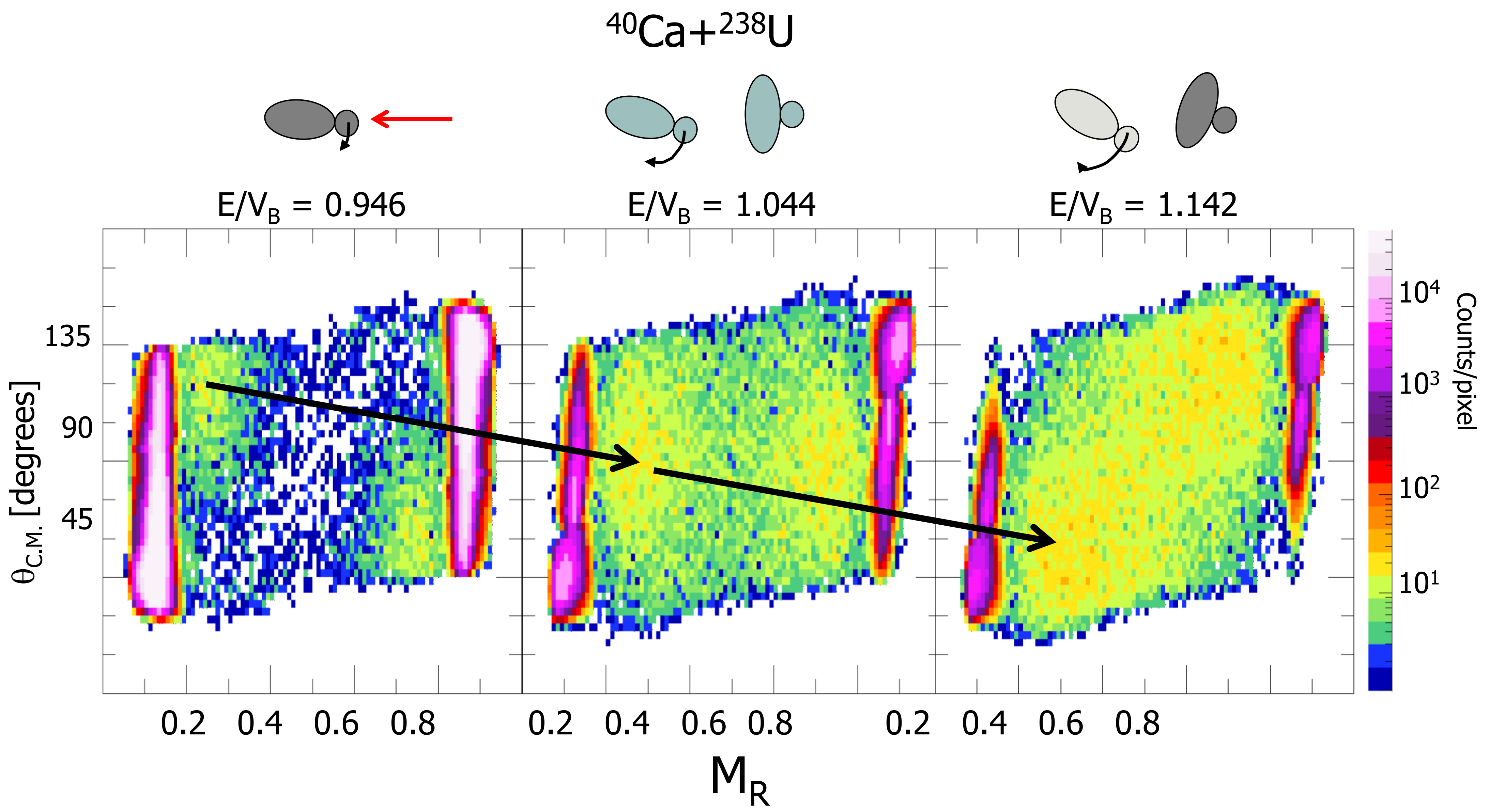

A. Wakhle et al., PRL **113** (2014) 182502

Fully-damped kinetic energy
(Viola+-20%)

K. Banerjee et al., submitted

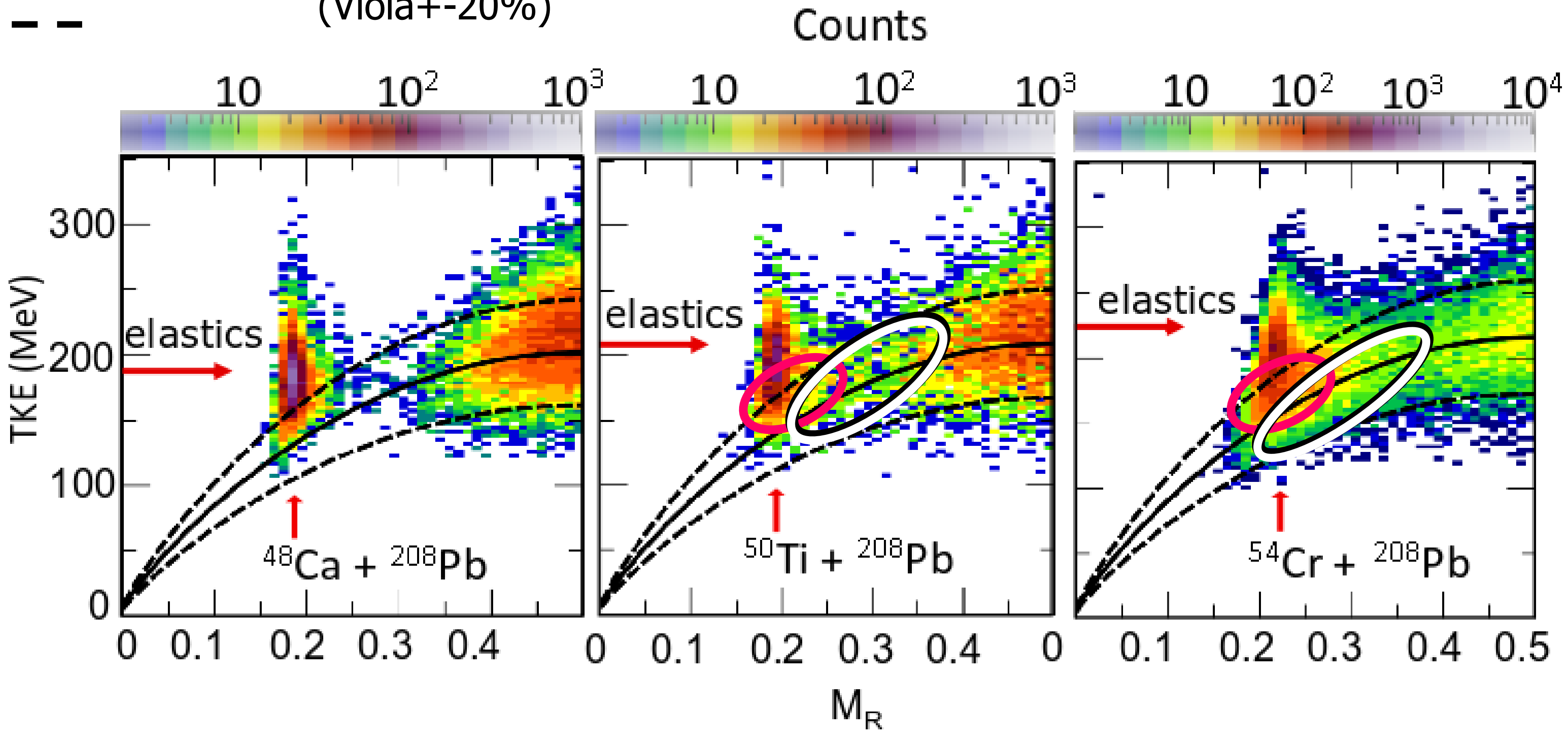

Increase in fast non-equilibrium processes as projectile charge increases:

Increasing deep-inelastic reactions (incomplete energy damping)

Increasing mass-asymmetric fast quasifission (full energy damping)

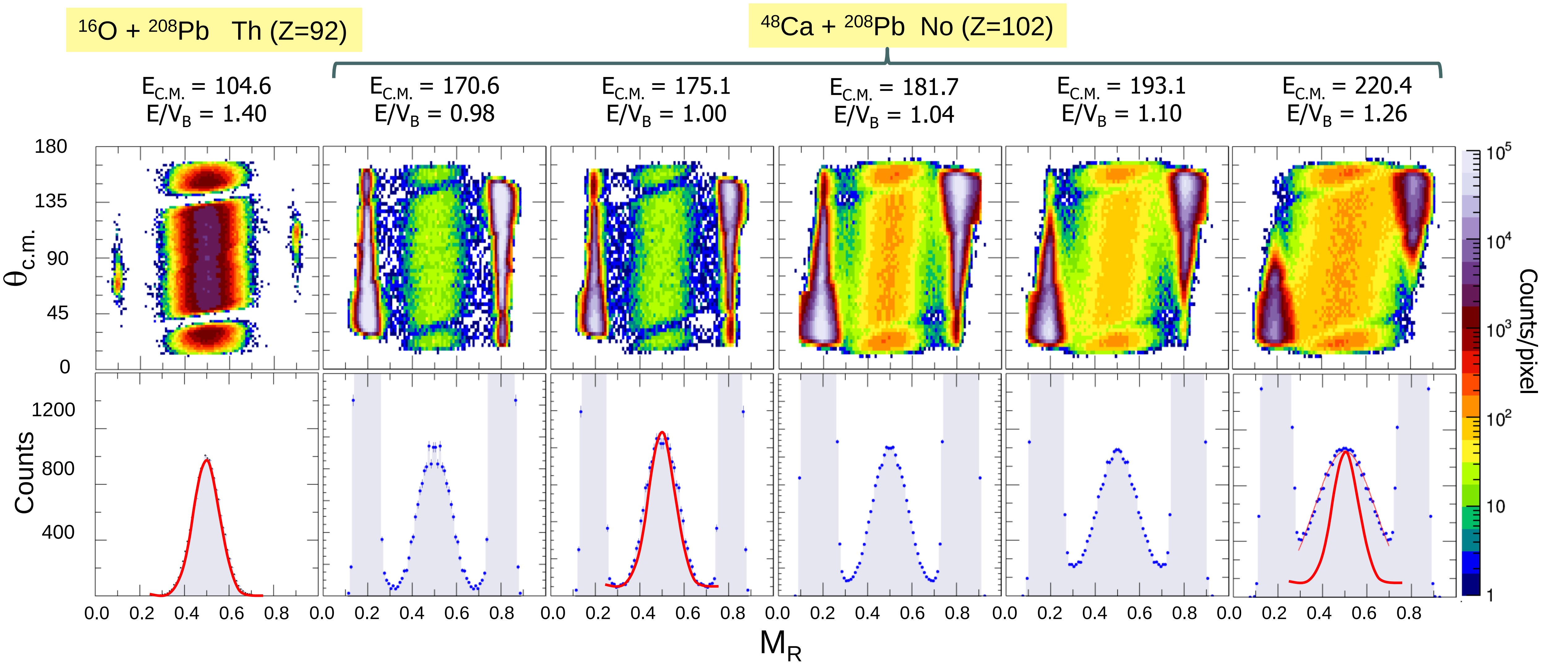
$^{16}O + {}^{208}Pb$ Th (Z=92)
$^{48}Ca + {}^{208}Pb$ No (Z=102)
$E_{C.M.} = 104.6$ $E/V_B = 1.40$
$E_{C.M.} = 170.6$ $E/V_B = 0.98$
$E_{C.M.} = 175.1$ $E/V_B = 1.00$
$E_{C.M.} = 181.7$ $E/V_B = 1.04$
$E_{C.M.} = 193.1$ $E/V_B = 1.10$
$E_{C.M.} = 220.4$ $E/V_B = 1.26$
$\theta_{c.m.}$
Counts
Counts/pixel
M_R

Effects of nuclear structure in the entrance channel:

Static deformation alignment

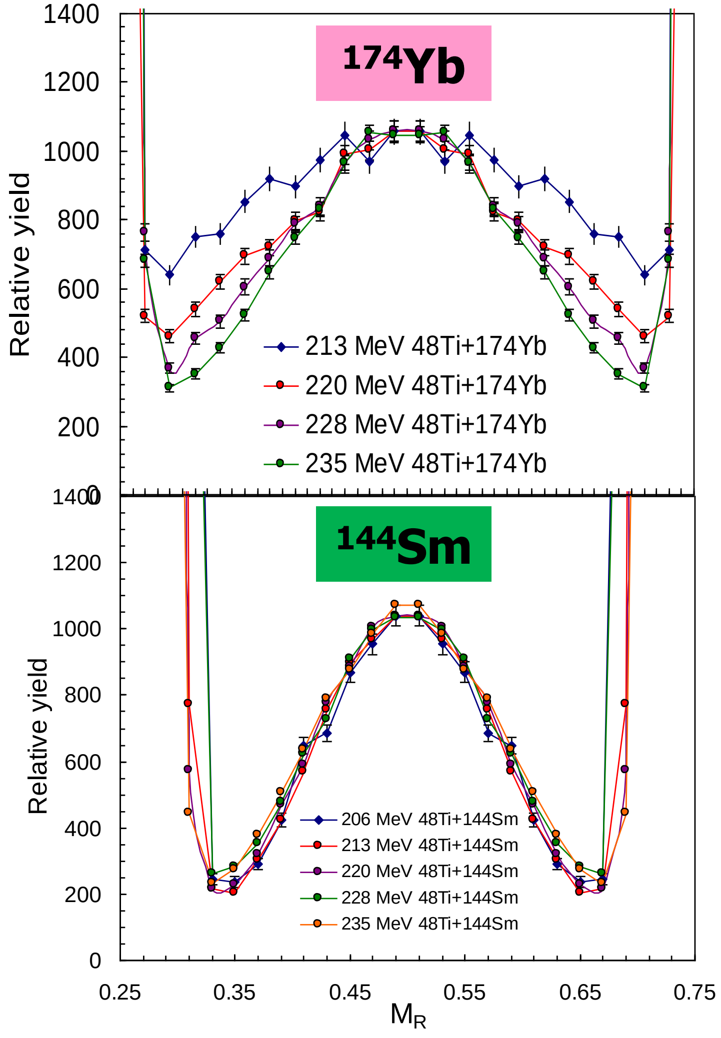

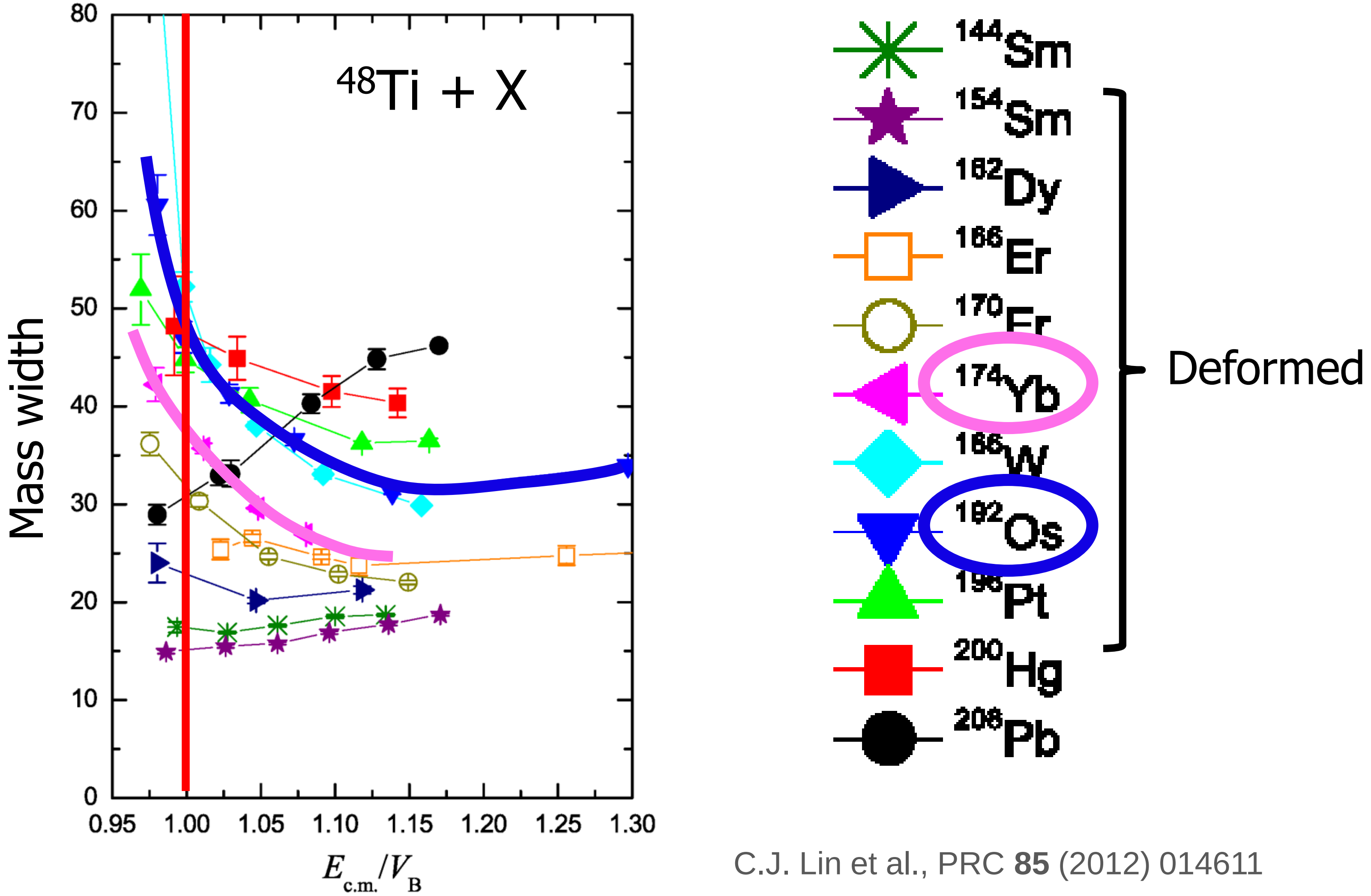

C.J. Lin et al., PRC **85** (2012) 014611

Consistent with measurements showing no/small ER σ sub-barrier

Mass-angle distributions – MAD

R. Bock et al., NP **A388** (1982) 334
J. Toke et al., NP **A440** (1985) 327
W.Q. Shen at al., PRC **36** (1987) 115
B.B. Back et al., PRC **53** (1996) 1734

GSI

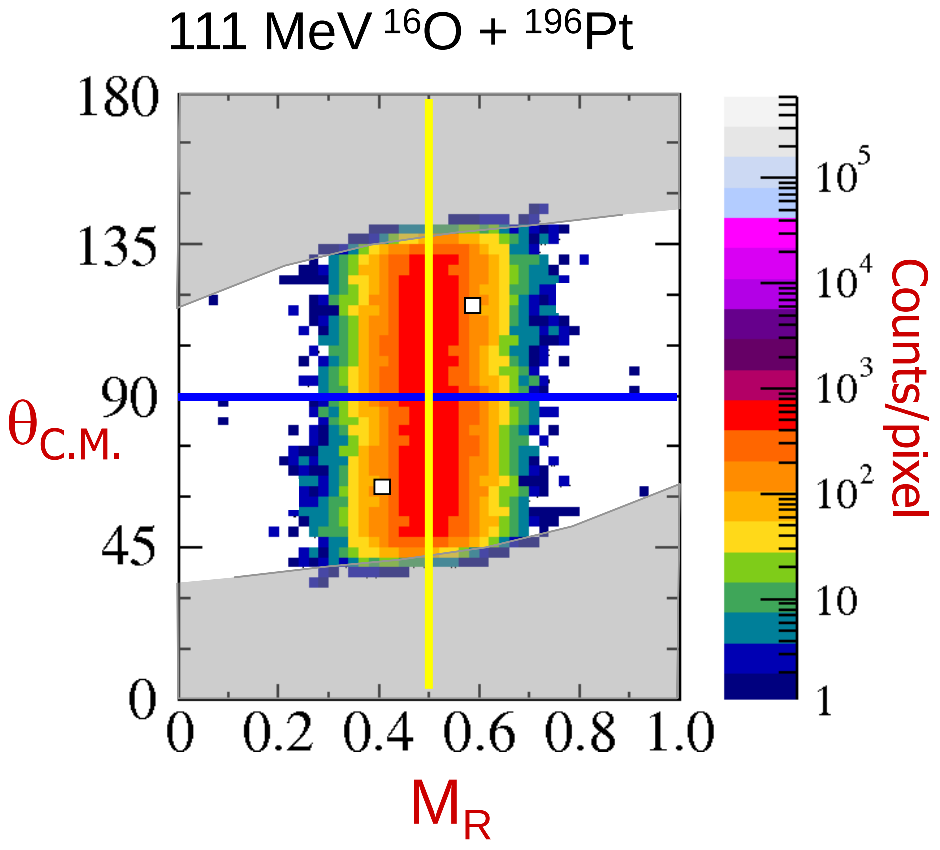

$^{54}Cr + ^{238}U$

$E/V_B = 0.98$ $E/V_B = 1.01$ $E/V_B = 1.02$

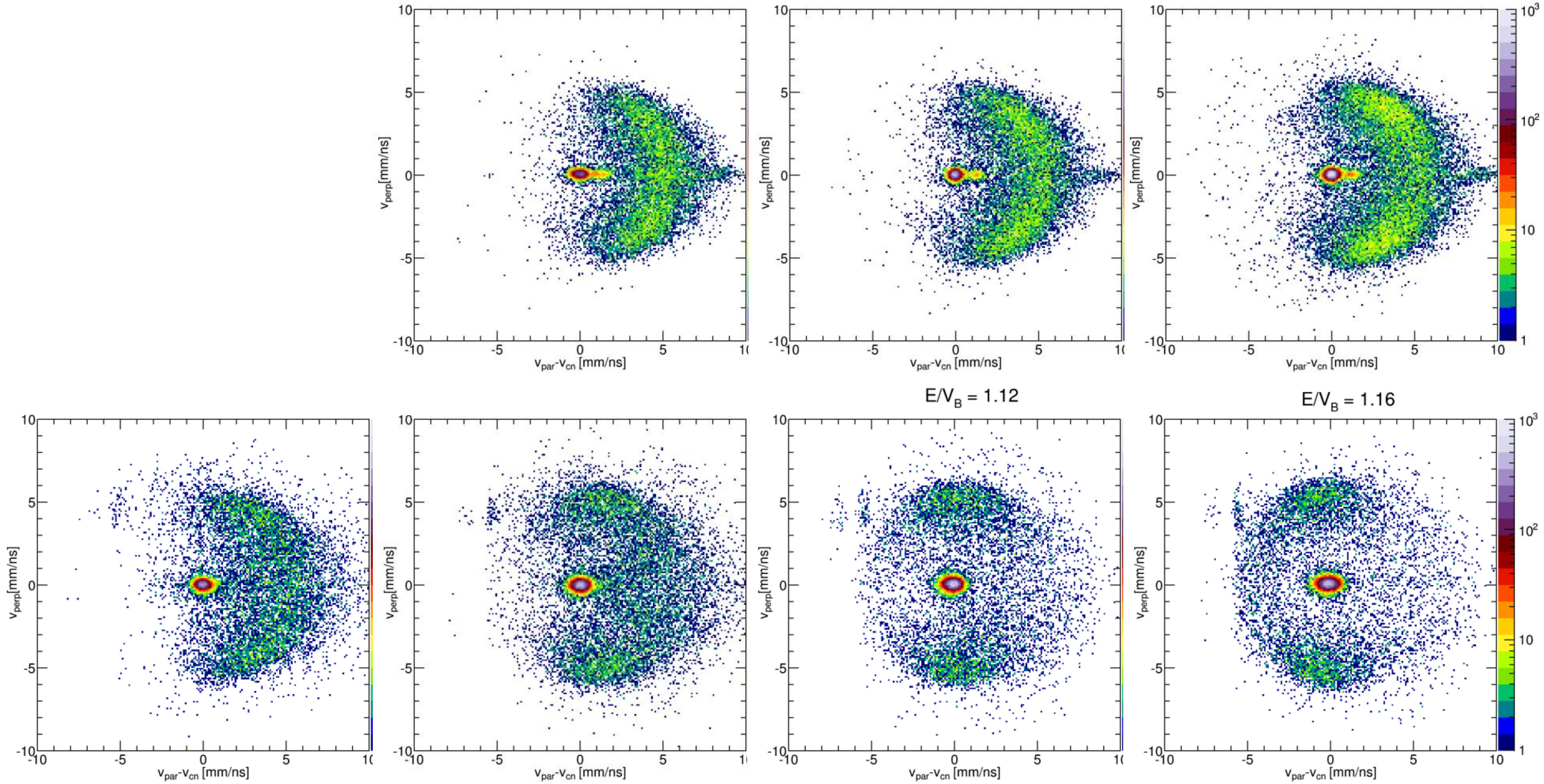

$E/V_B = 1.04$ $E/V_B = 1.08$ $E/V_B = 1.12$ $E/V_B = 1.16$

Two modes of quasi-fission – effect of deformation alignment

Hinde et al., PR **C53** (1996) 1290

$^{32}S + ^{232}Th$ (prolate)

^{232}Th: fissile – fission after peripheral collisions

Elimination of non-binary events: co-linear in c.m. frame

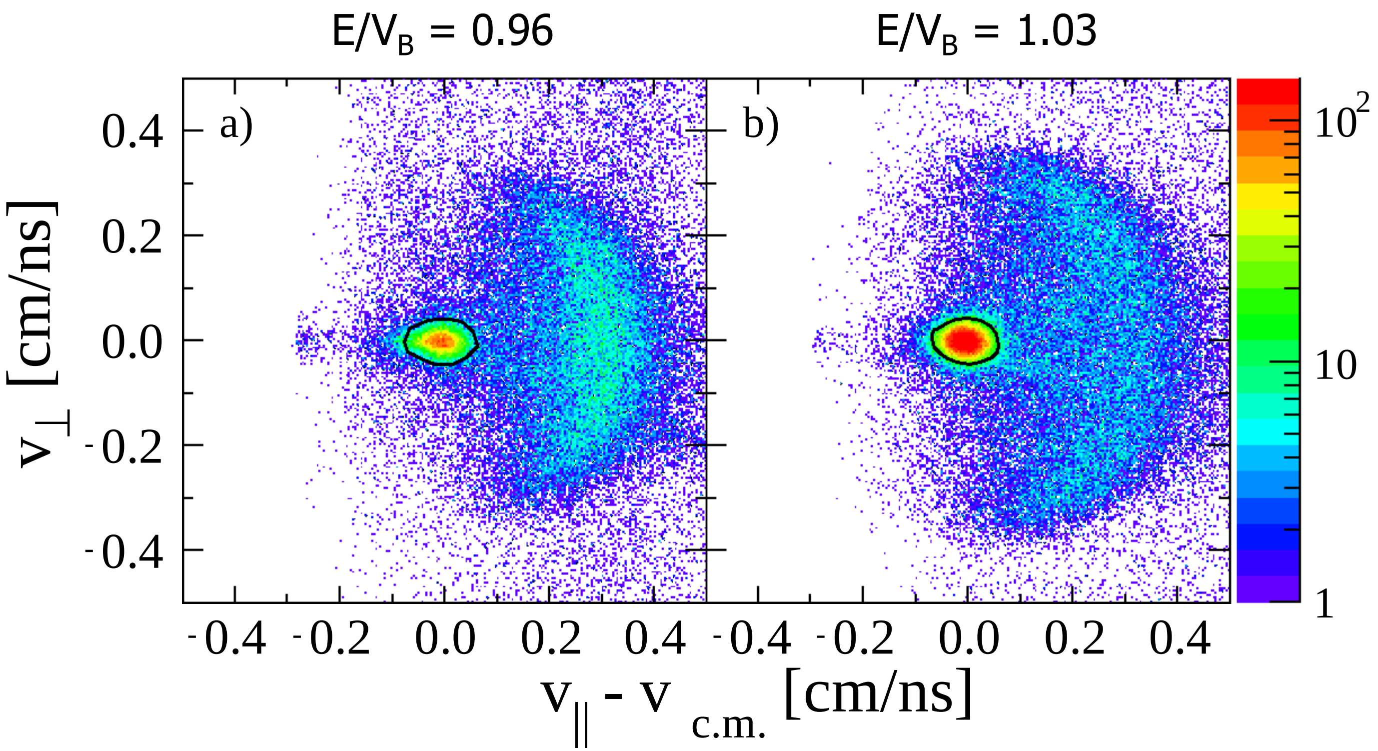

MAD: $^{32}S + ^{232}Th$

Hinde et al., PRL **101** (2008) 092702

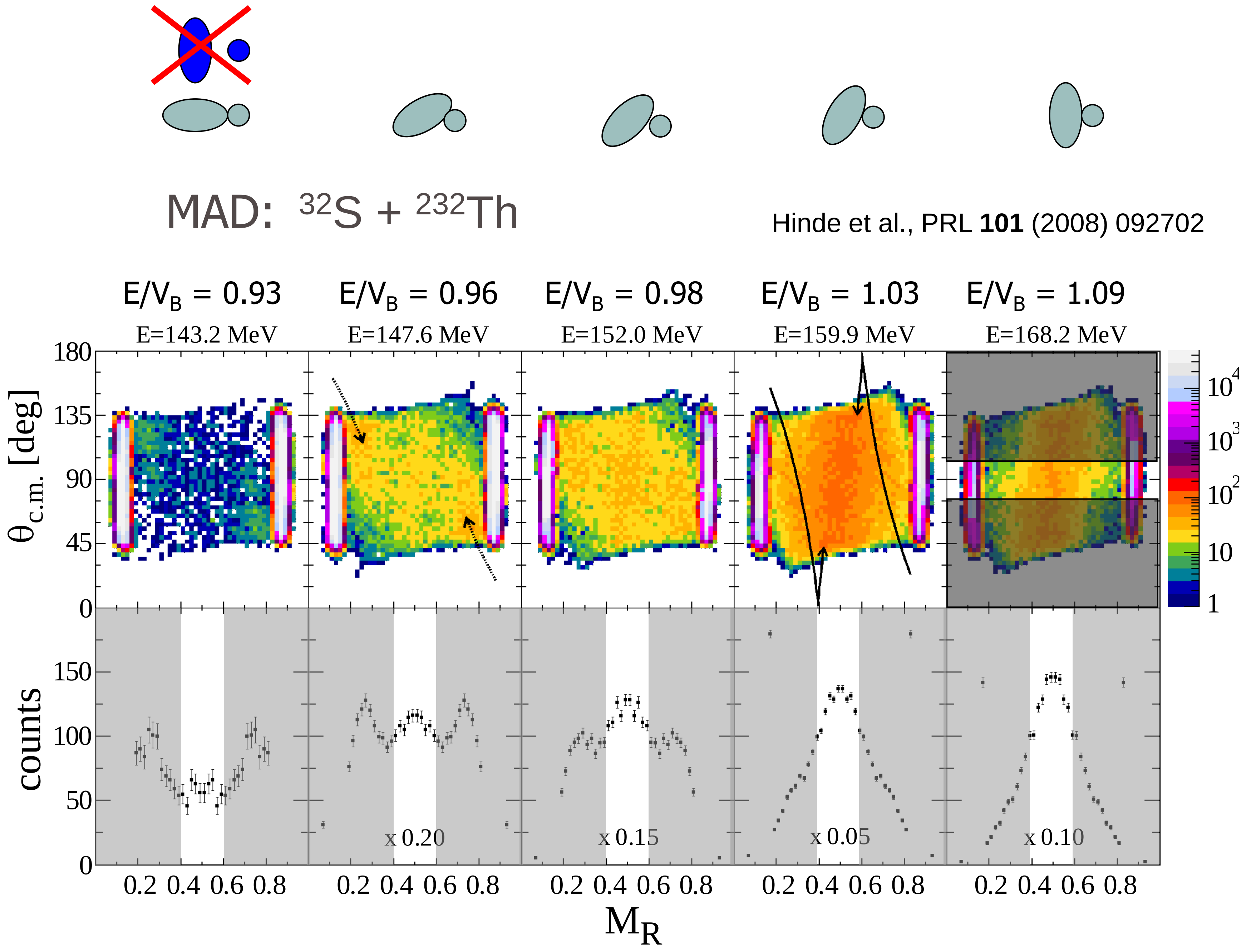

Mass-symmetric fragment angular anisotropies

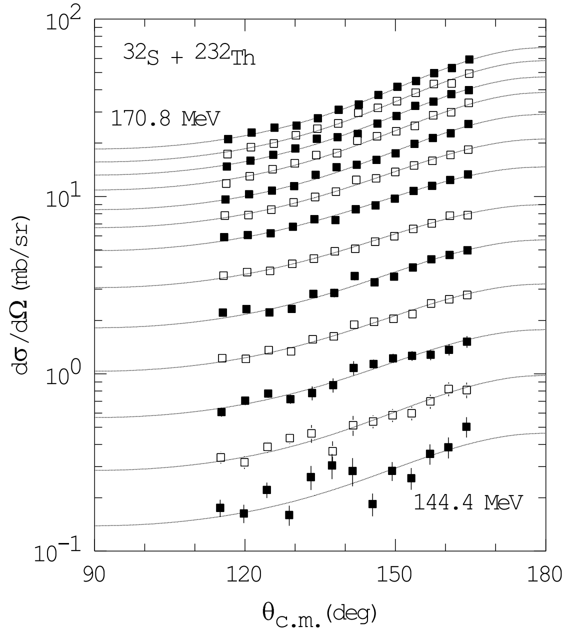

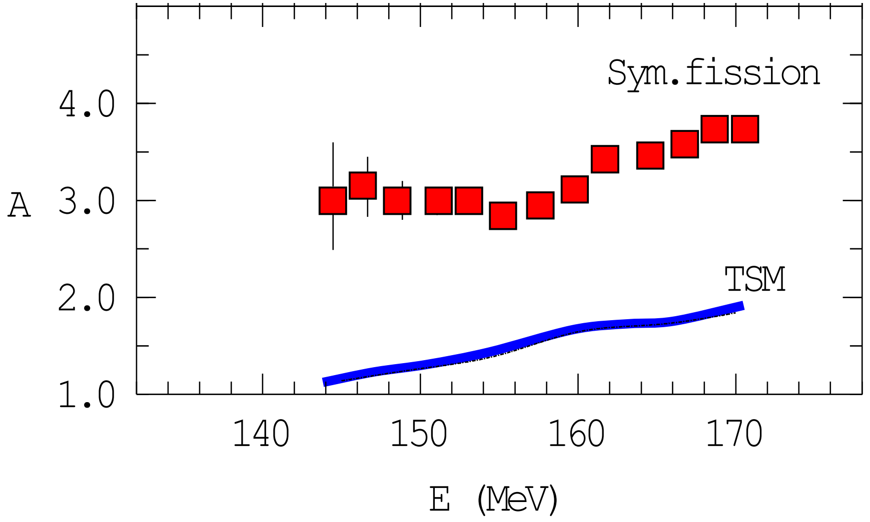

Hinde et al., J.Nucl.Radiochem.Sci. **3** (2002) 31
Hinde et al., PRL **101** (2008) 092702

- Mass-symmetric component shows large angular anisotropies – QF!

  Supports previous interpretation of deformation alignment effect on dynamics deduced from similar anisotropy results for $^{16}O + ^{238}U$

  Hinde et al., PRL **74** (1995) 1295; Hinde et al., PRC **53** (1996) 1290

MAD – time scales of mass-equilibration and rotation (GSI)

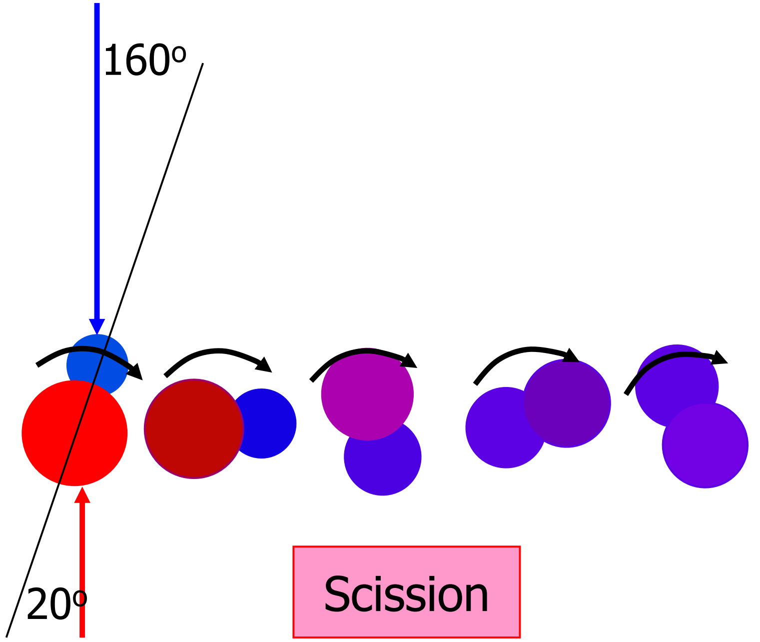

R. Bock et al., NP **A388** (1982) 334
J. Toke et al., NP **A440** (1985) 327
W.Q. Shen at al., PRC **36** (1987) 115
B.B. Back et al., PRC **53** (1996) 1734

Miminal mass-angle correlation

Strong mass-angle correlation

QF Timescales from MAD

Experimental MAD

Counts/pixel

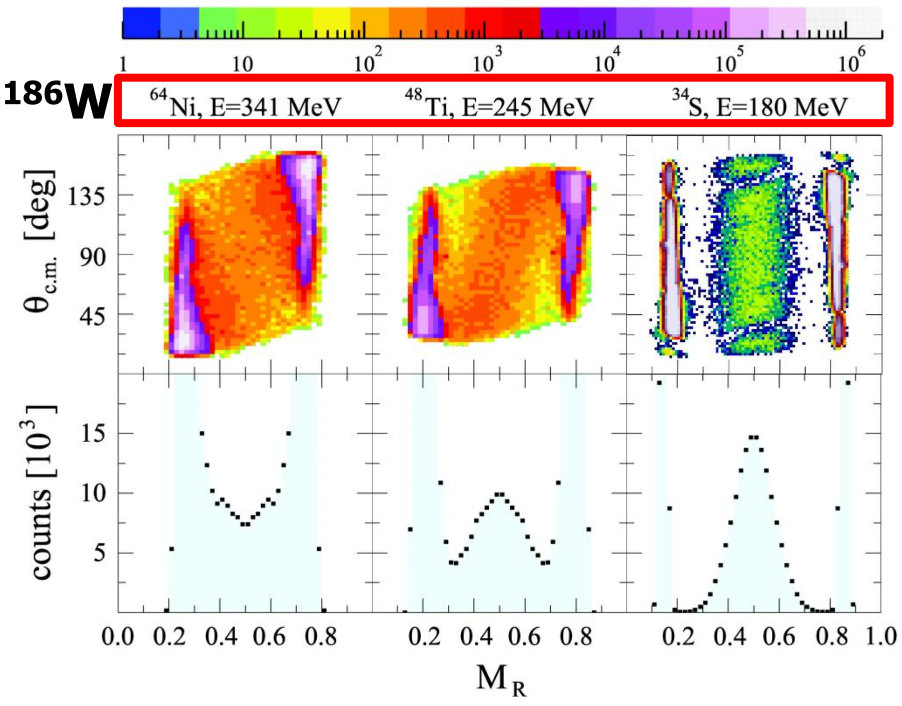

R. du Rietz et al. PRL **106** (2011) 052701

R. du Rietz et al., PRC **88** (2013) 054618

MAD Map

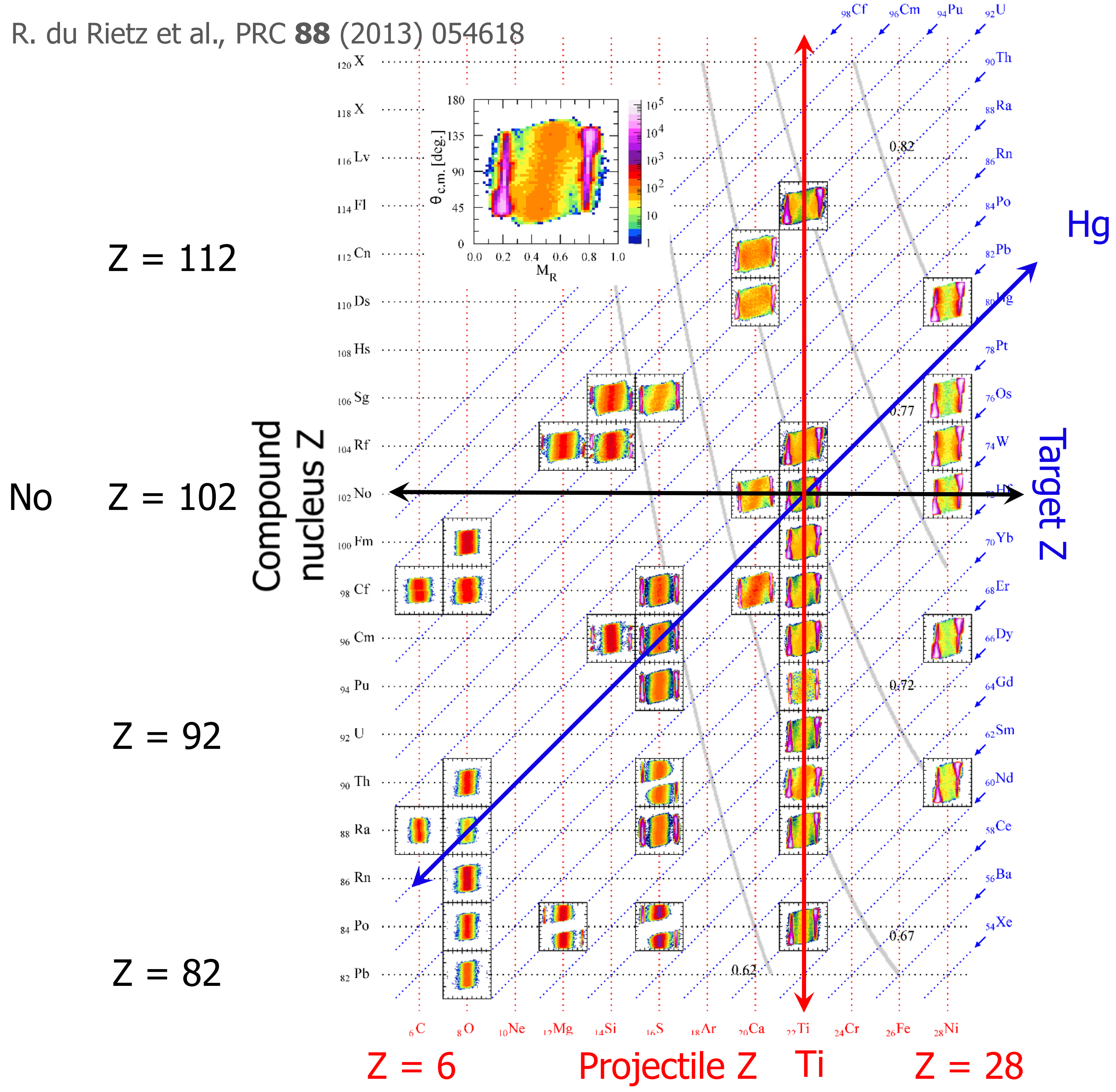

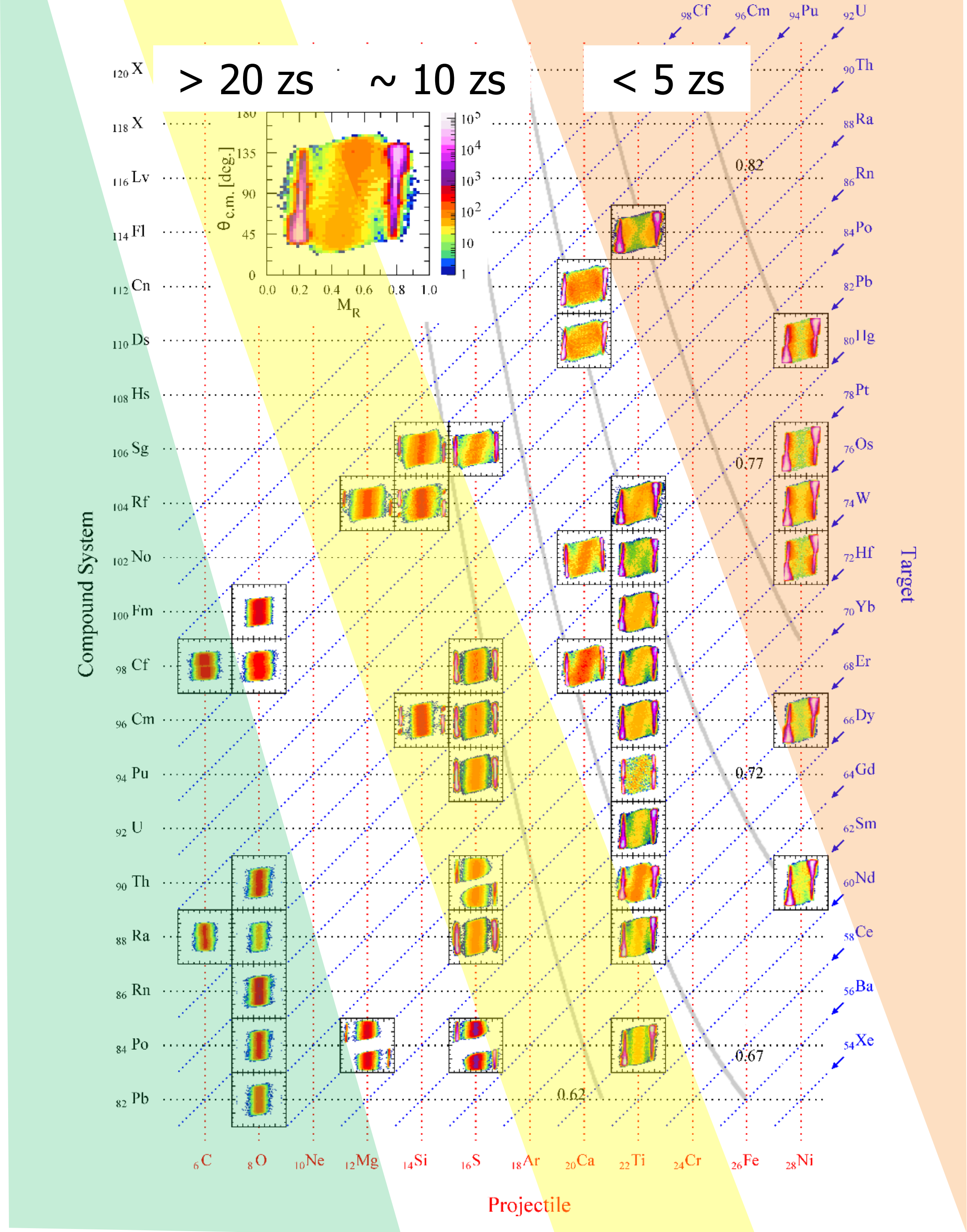

> 20 zs
~ 10 zs
< 5 zs
Compound System
Projectile
Target
θc.m. [deg.]
MR
0.82
0.77
0.72
0.67
0.62
120 X
118 X
116 Lv
114 Fl
112 Cn
110 Ds
108 Hs
106 Sg
104 Rf
102 No
100 Fm
98 Cf
96 Cm
94 Pu
92 U
90 Th
88 Ra
86 Rn
84 Po
82 Pb
6 C
8 O
10 Ne
12 Mg
14 Si
16 S
18 Ar
20 Ca
22 Ti
24 Cr
26 Fe
28 Ni
98 Cf
96 Cm
94 Pu
92 U
90 Th
88 Ra
86 Rn
84 Po
82 Pb
80 Hg
78 Pt
76 Os
74 W
72 Hf
70 Yb
68 Er
66 Dy
64 Gd
62 Sm
60 Nd
58 Ce
56 Ba
54 Xe

COLD FUSION

Sub-barrier MAGIC

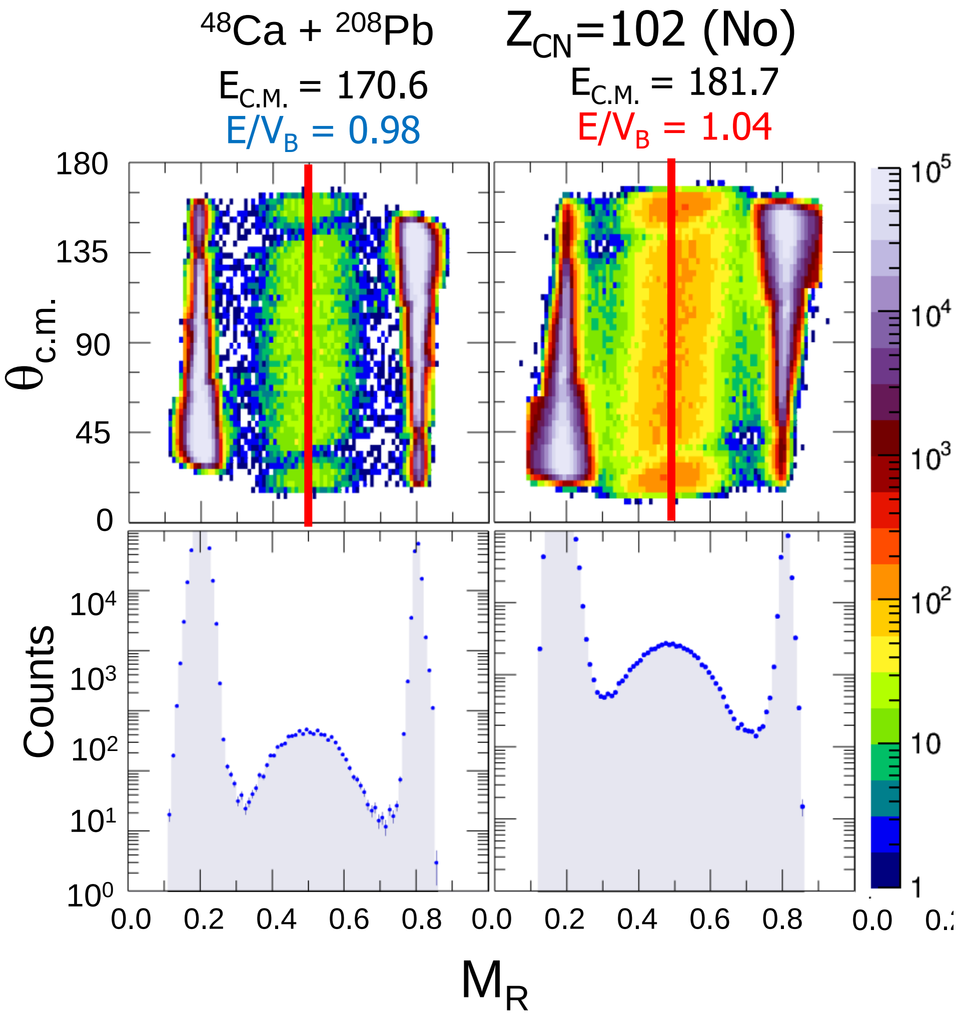

"HOT" FUSION reactions with prolate deformed actinide target nuclei

ANU: Th, U targets; Mainz/GSI: Pu, Cm, Cf targets

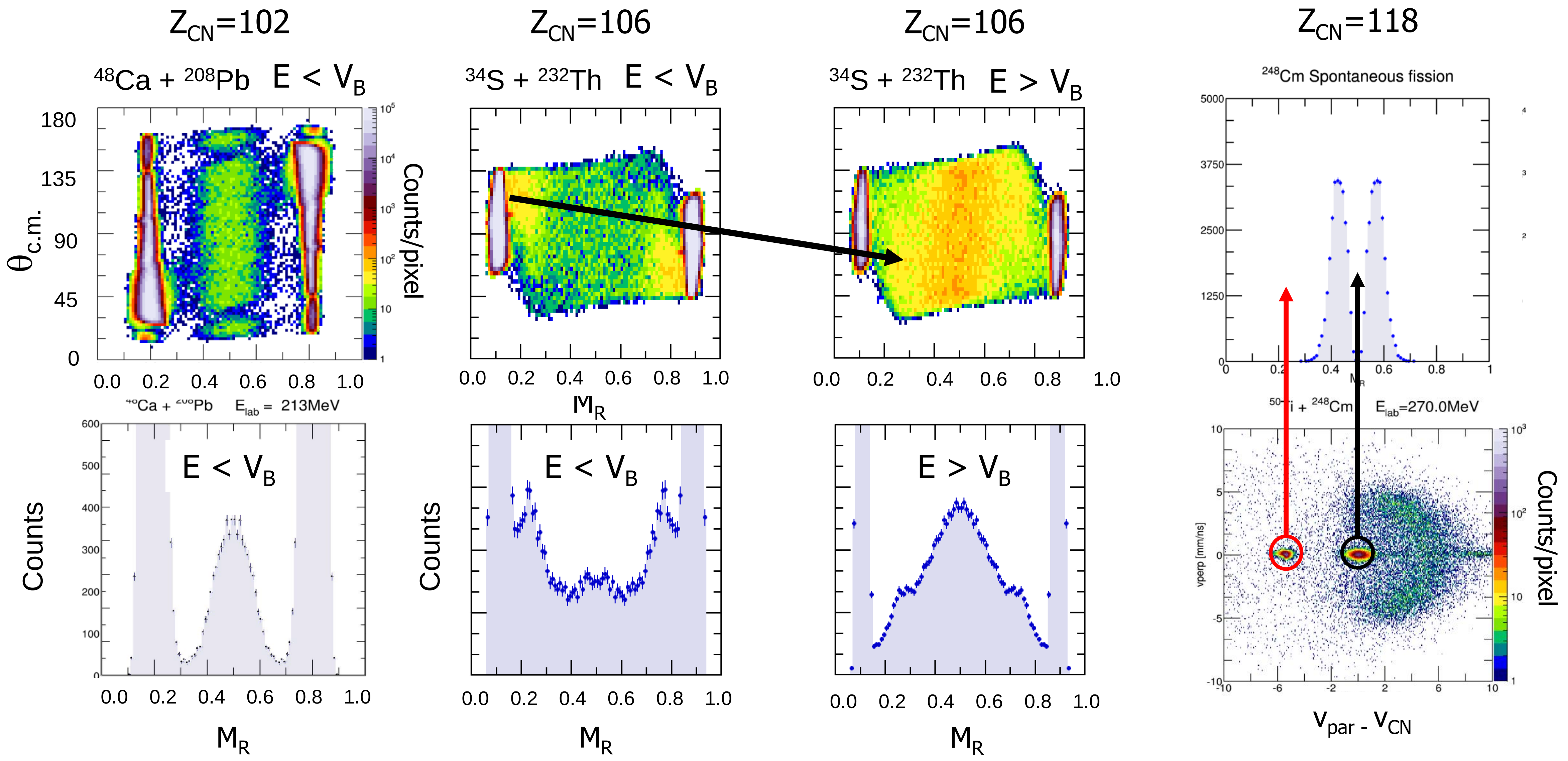

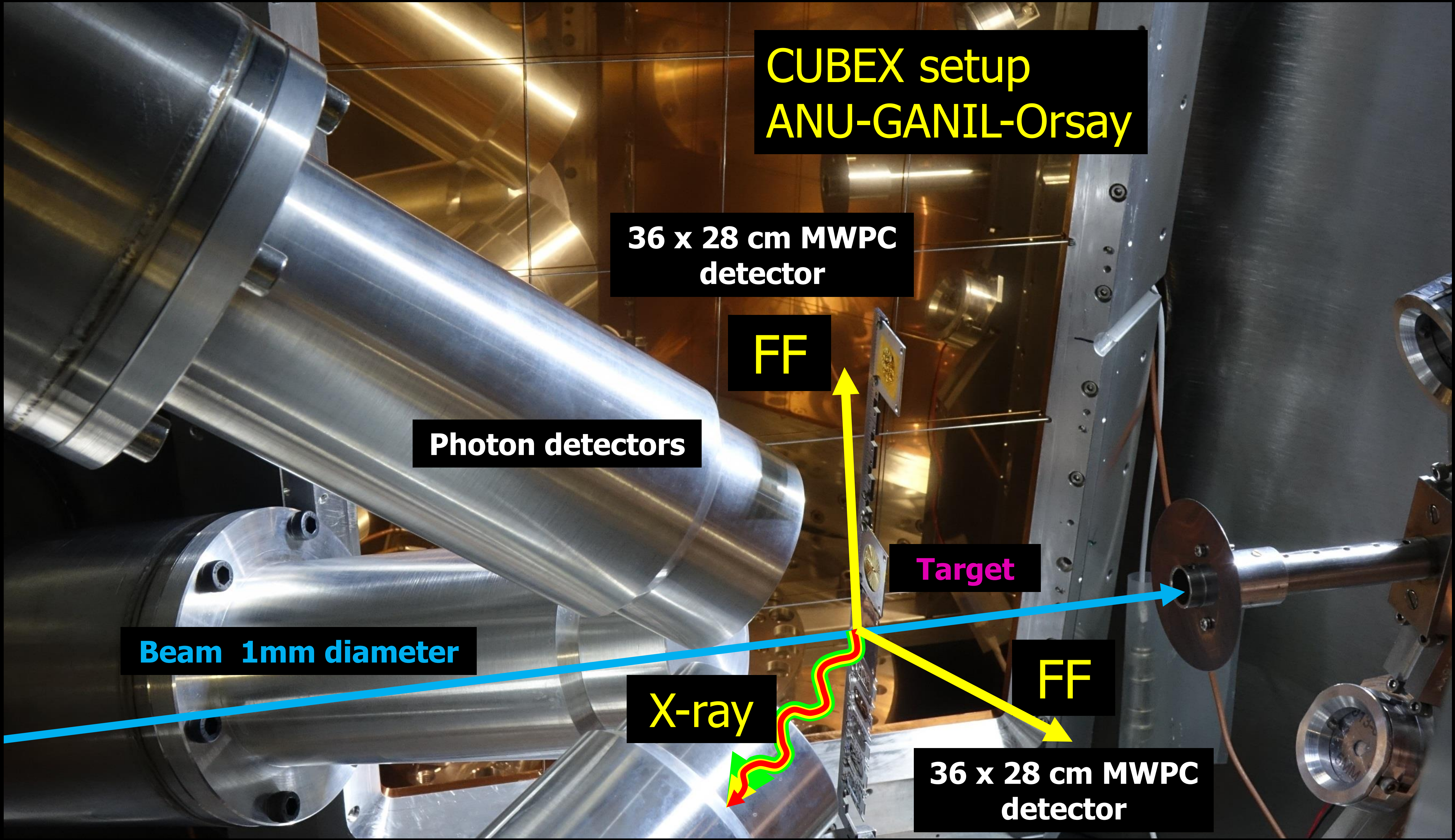
CUBEX setup
ANU-GANIL-Orsay
36 x 28 cm MWPC detector
FF
Photon detectors
Target
Beam 1mm diameter
X-ray
FF
36 x 28 cm MWPC detector

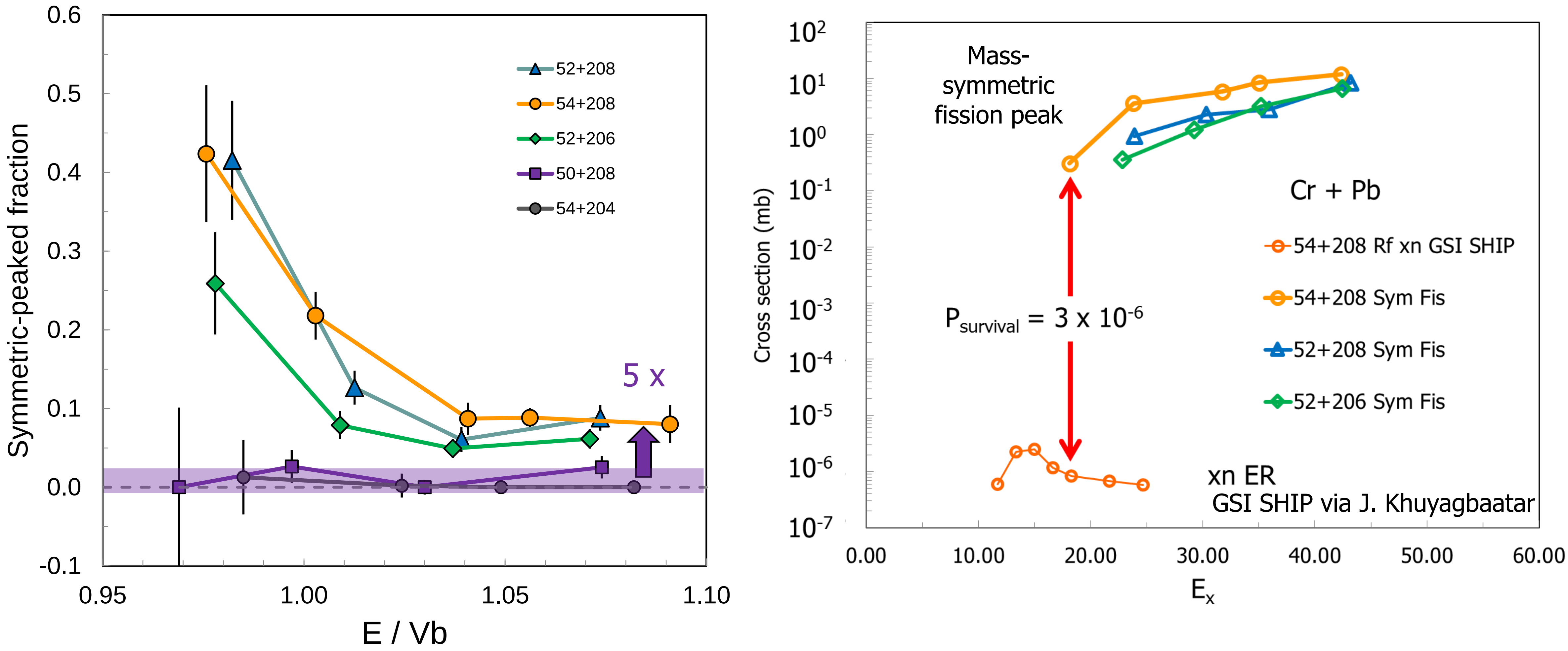

Mass-symmetric and mass-asymmetric – trajectory bifurcation

Mass-symmetric component is narrow – fusion fission?

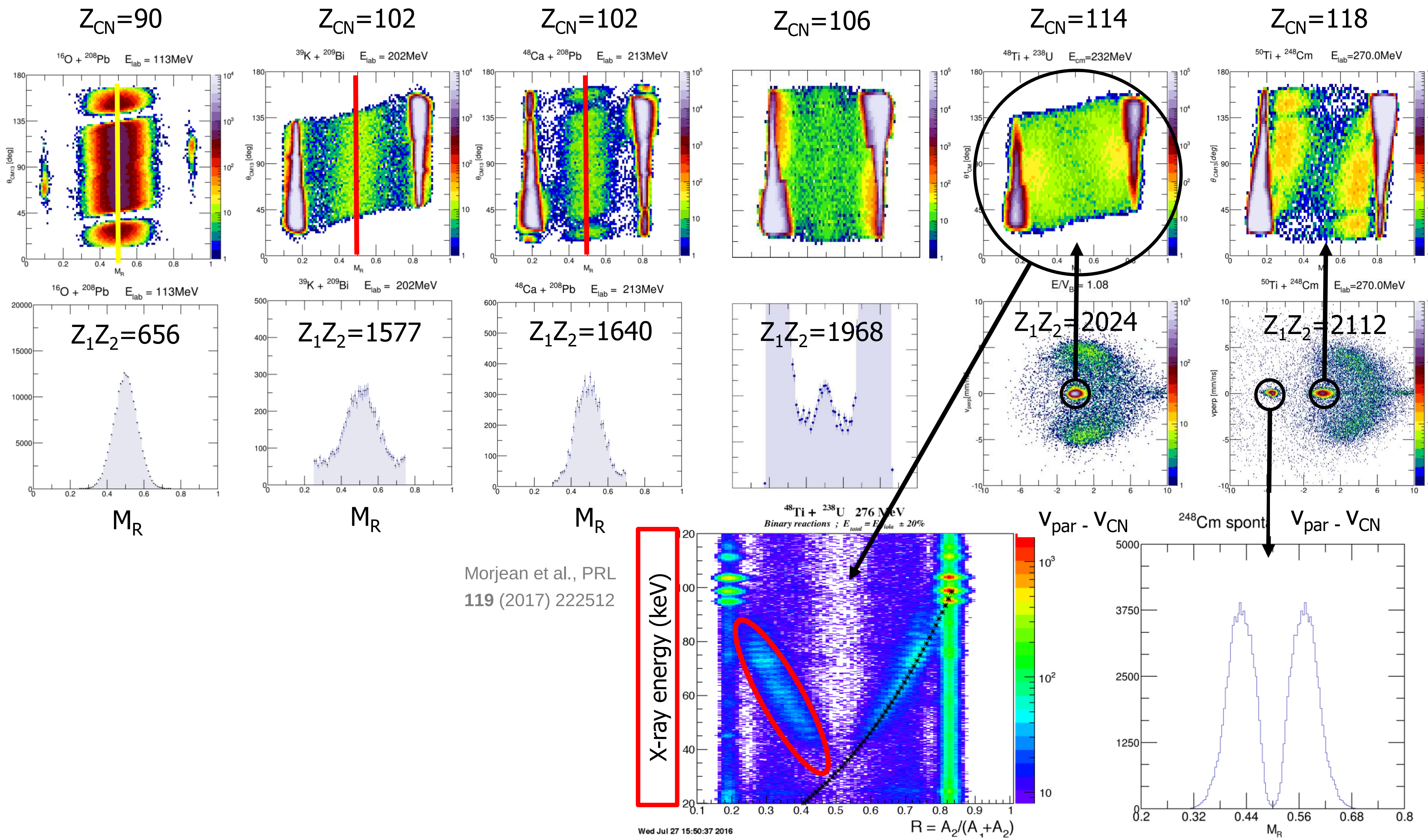
Z_CN=90
Z_CN=102
Z_CN=102
Z_CN=106
Z_CN=114
Z_CN=118
16O + 208Pb E_lab = 113MeV
39K + 209Bi E_lab = 202MeV
48Ca + 208Pb E_lab = 213MeV
48Ti + 238U E_cm=232MeV
50Ti + 248Cm E_lab=270.0MeV
Z1Z2=656
Z1Z2=1577
Z1Z2=1640
Z1Z2=1968
Z1Z2=2024
Z1Z2=2112
E/V_B = 1.08
M_R
M_R
M_R
V_par - V_CN
V_par - V_CN
48Ti + 238U 276 MeV
Binary reactions ; E_total = E_Viola ± 20%
X-ray energy (keV)
R = A2/(A1+A2)
Wed Jul 27 15:50:37 2016
248Cm spont.
M_R
Morjean et al., PRL 119 (2017) 222512

Spherical magic nuclei and N/Z matching

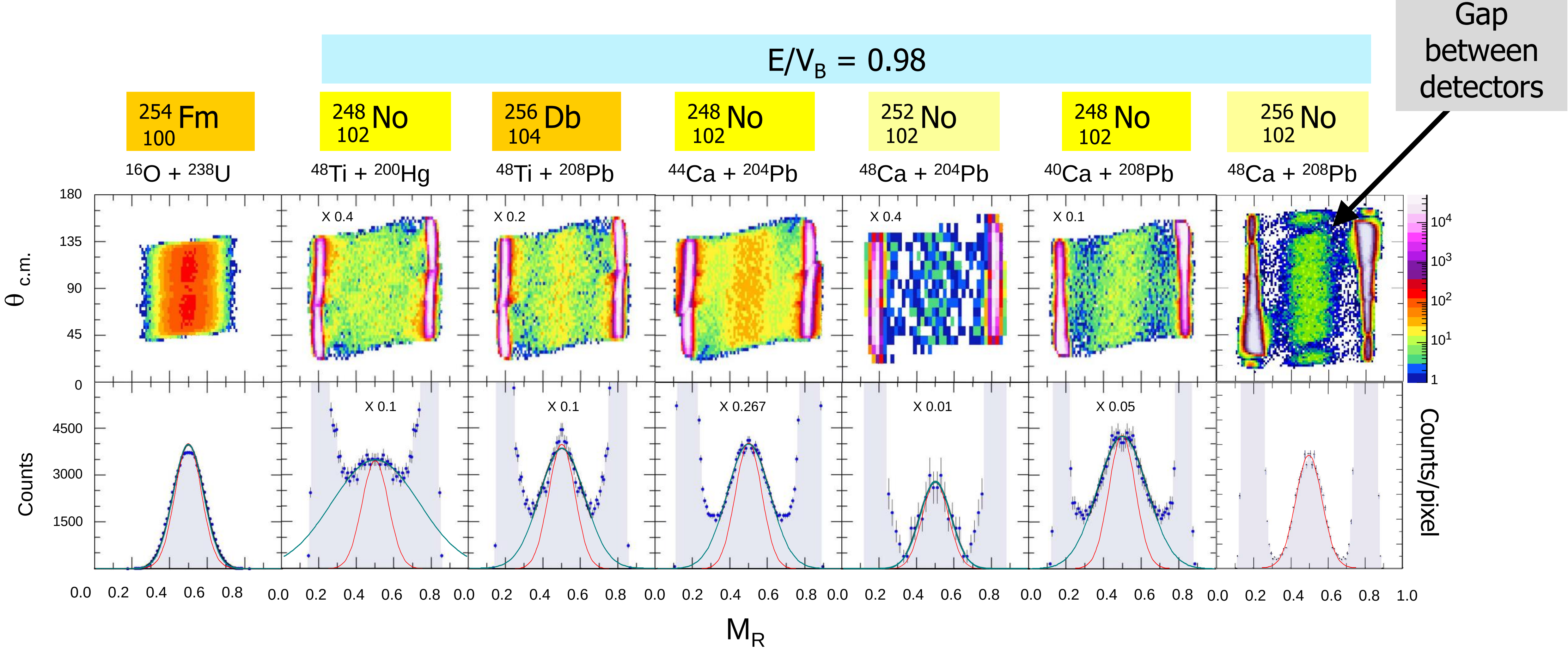

N_{magic}	2	0	2	2	3	4	4
$\Delta(N/Z)$	0.57	0.32	0.35	0.29	0.09	0.54	0.14

C. Simenel et al., PLB 710 (2012) 607 E. Prokhorova et al., NP A802(2008)45 D.Y. Jeong, T. Valentini et al., ANU, unpublished

Entrance channel closed shells and N/Z mismatch

N/Z equilibration will cause early energy damping as nuclei overlap:

- more elongated "entry point" to diffusive motion

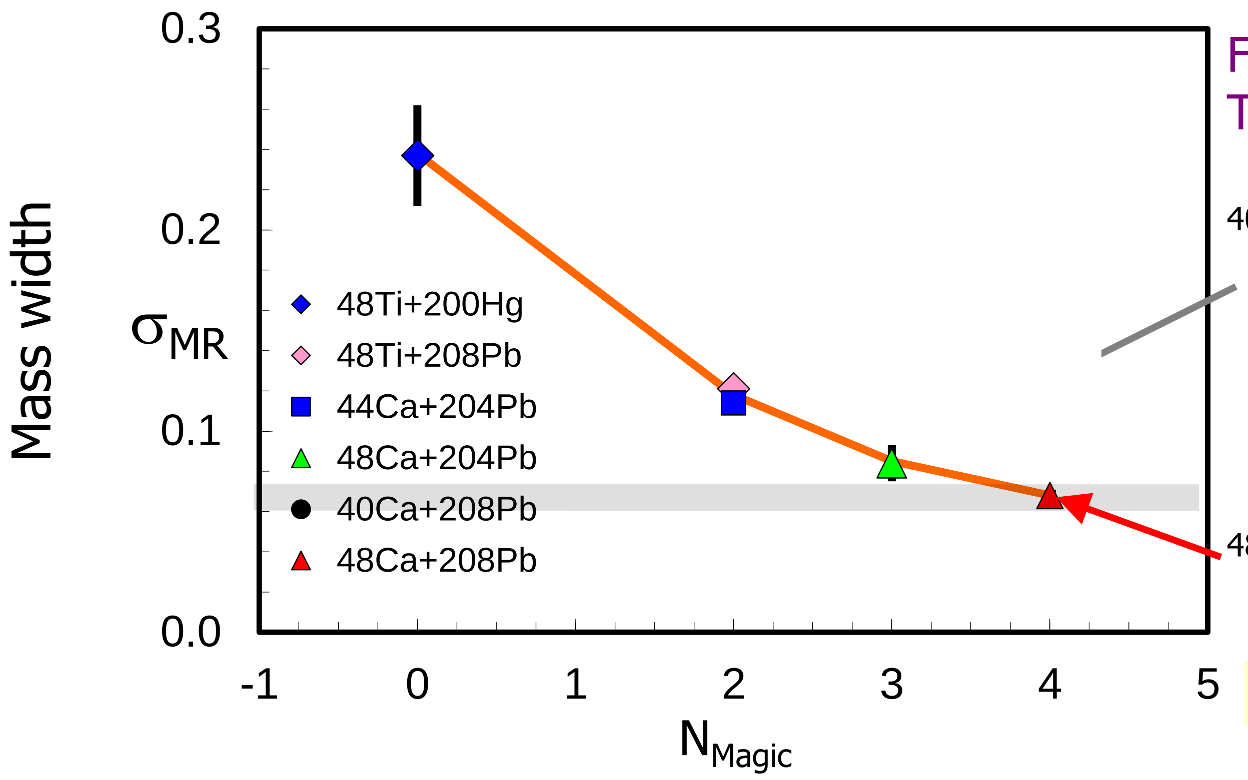

Fast N/Z equilibration.
TDHF calculated outcomes:

^{40}Ca+^{208}Pb
P(no transfer) ~ 10^{-4}

Average transfer outcome:
^{42}Ar+ ^{206}Po $N_m = 0$

^{48}Ca+^{208}Pb
P(no transfer) ~ 0.5

C. Simenel et al., PLB 710 (2012) 607

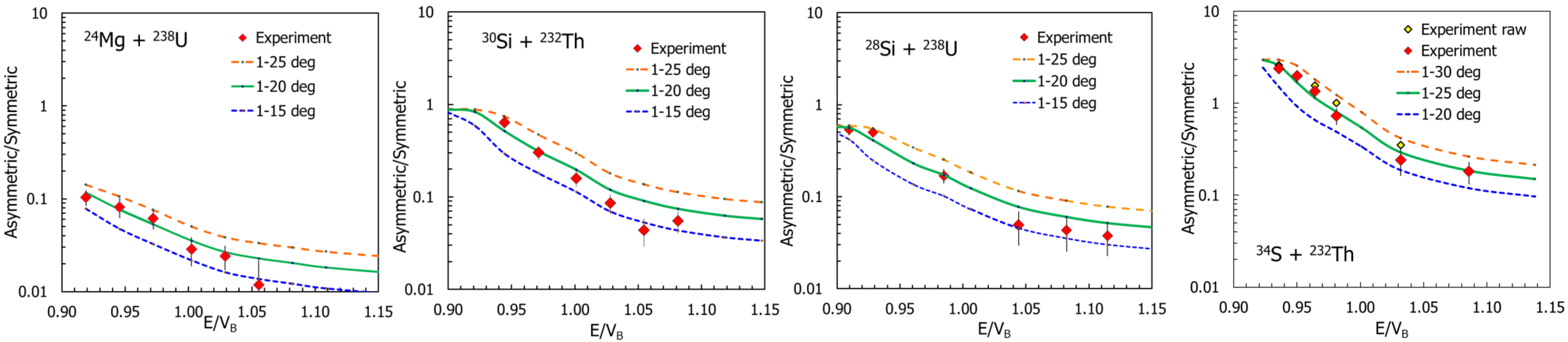

$^{24}Mg + ^{238}U$
Experiment
1-25 deg
1-20 deg
1-15 deg
Asymmetric/Symmetric
E/V$_B$
$^{30}Si + ^{232}Th$
Experiment
1-25 deg
1-20 deg
1-15 deg
Asymmetric/Symmetric
E/V$_B$
$^{28}Si + ^{238}U$
Experiment
1-25 deg
1-20 deg
1-15 deg
Asymmetric/Symmetric
E/V$_B$
Experiment raw
Experiment
1-30 deg
1-25 deg
1-20 deg
$^{34}S + ^{232}Th$
Asymmetric/Symmetric
E/V$_B$

Mass-symmetric fission fragment angular distributions

- Mass-symmetric component shows large angular anisotropies – QF (B.B. Back 1983)

$^{32}S + ^{232}Th$

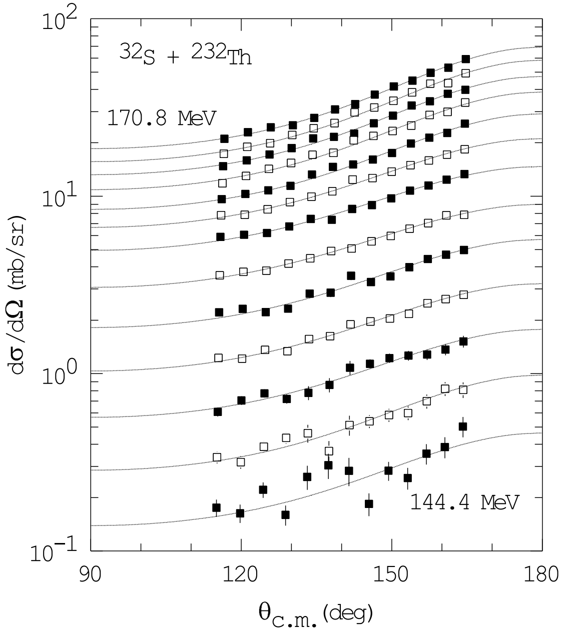

Hinde et al., J. Nucl. Radiochem. Sci. **3** (2002) 31
Hinde et al., PRL **101** (2008) 092702

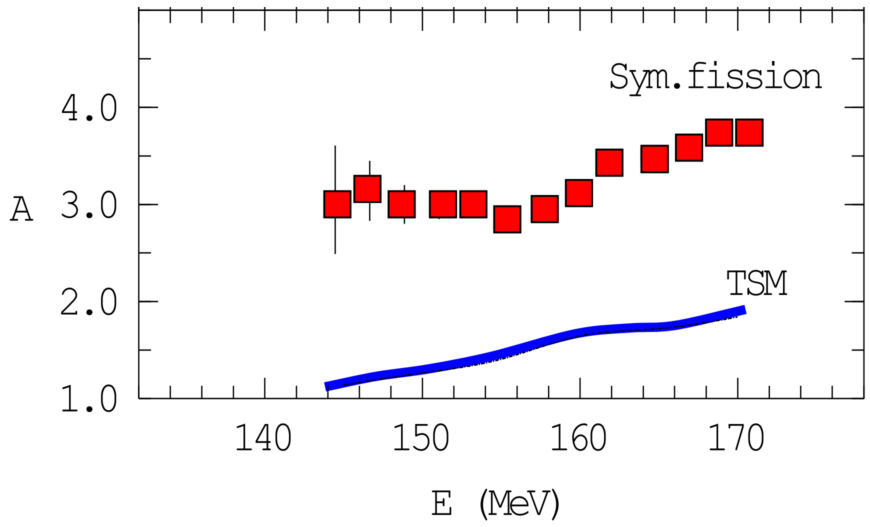

Mass-symmetric fission fragment angular distributions

- Mass-symmetric component shows large angular anisotropies – QF (B.B. Back 1983)

$^{32}S + ^{232}Th$

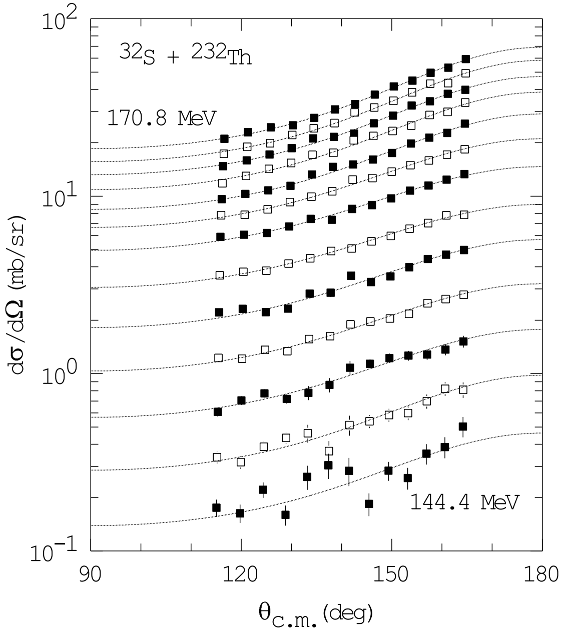

Hinde et al., J. Nucl. Radiochem. Sci. **3** (2002) 31
Hinde et al., PRL **101** (2008) 092702

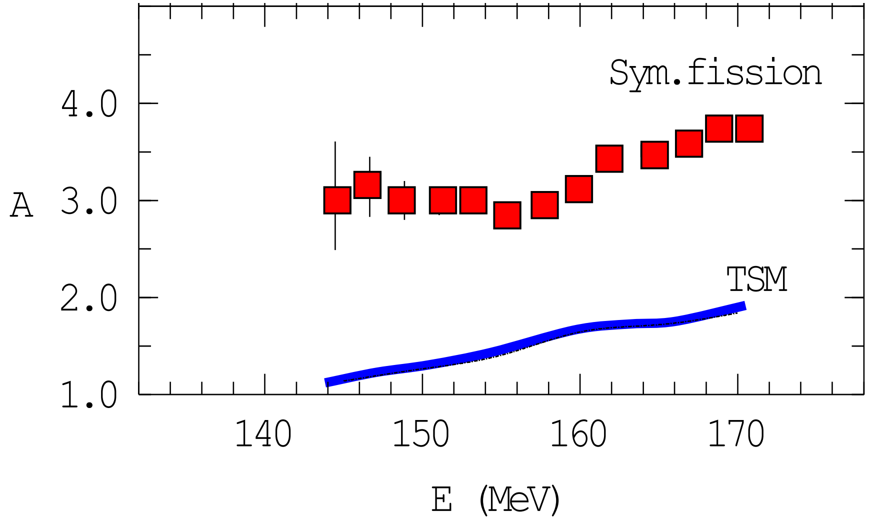

Conclusion from measured beam energy dependence of $^{16}O + ^{238}U$ angular anisotropies:

"In attempting to form very fissile nuclei near their equilibrium deformation, only reactions associated with passage over the highest fusion barriers can result in the compact shapes which lead to the survival of evaporation residues."

PRL **74** (1995) 1295

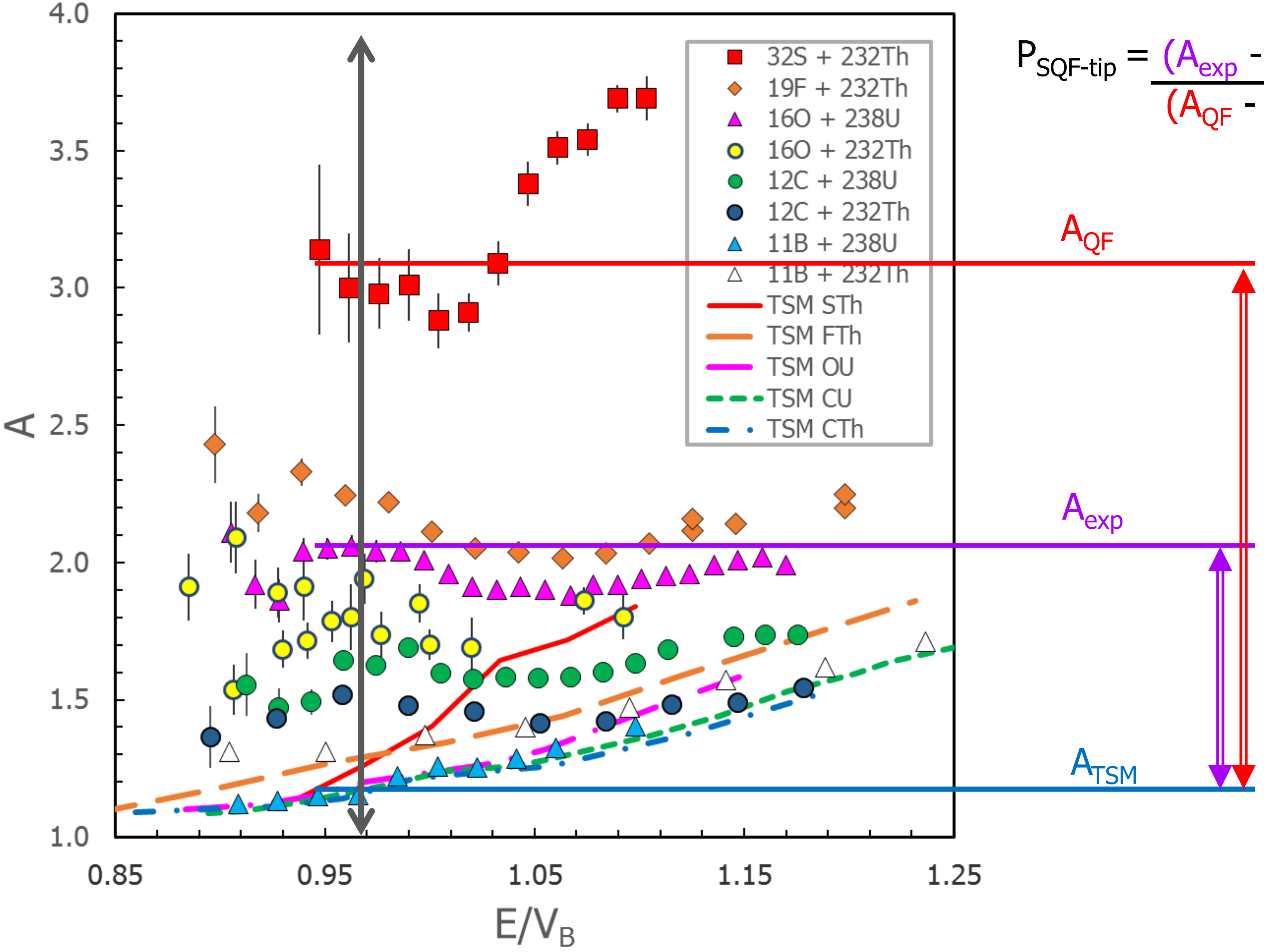

$$P_{SQF\text{-}tip} = \frac{(A_{exp} - A_{TSM})}{(A_{QF} - A_{TSM})}$$

Defining smooth liquid drop QF dynamics

- minimise shell effects – high Ex – high E/V_b
- minimise effects of angular momentum – low E/V_b
- Compromise: choose E/V_b = 1.05-1.10
  - effects of spherical magic numbers attenuated by Ex
  - effects of deformation alignment averaged out
  - in angular momentum regime relevant to SHE production

Dependence of quasifission probability and characteristics (time scale) on collision variables (related to P_{CN}):

- Compound nucleus fissility (Z^2/A);
- Coulomb repulsion (Z_1Z_2);
- Angular momentum;
- Nuclear structure of the colliding nuclei:
  - deformation
  - closed shells (magic numbers)

Many variables!

Analogy between QF dynamics and nuclear masses

- Smooth liquid drop dynamics (Coulomb, nuclear, viscosity)
- Modification of dynamics due to shell structure (PES and viscosity)

Ultimate goal: reliable model including all relevant physics to predict P_{CN}

Model should predict QF characteristics, as QF is most likely outcome

Defining smooth "liquid drop" QF dynamics

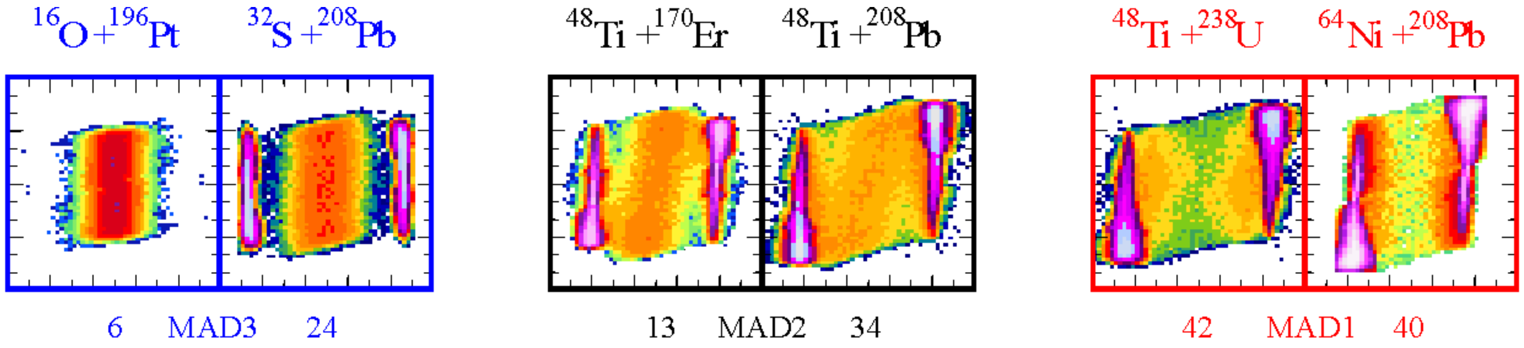

$E/V_B = 1.05\text{-}1.10$

- effects of spherical magic numbers attenuated by Ex
- deformation effects averaged out
- dynamics not dominated by high angular momentum

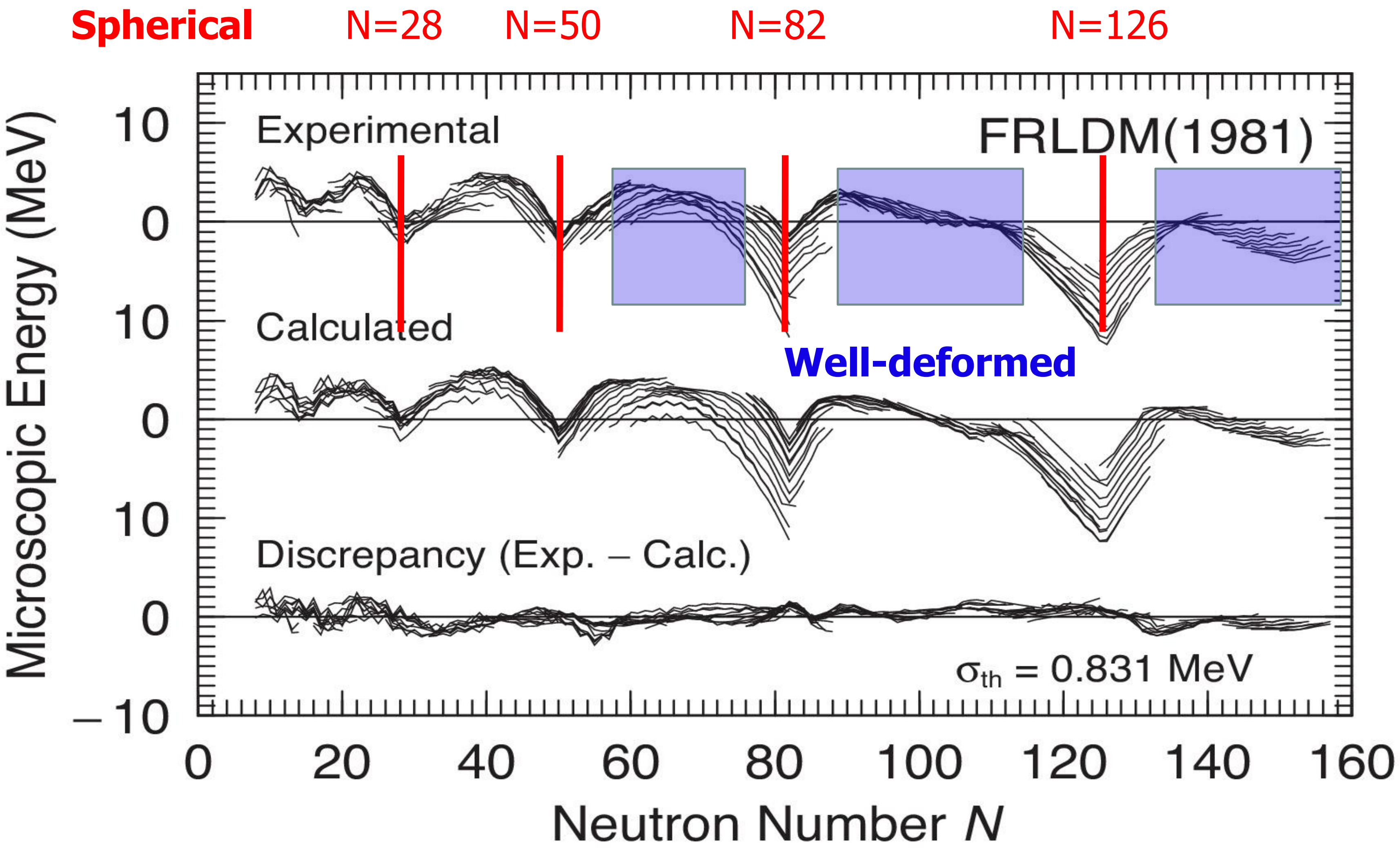

Fig. 1 Differences between experimental masses and a recent macroscopic (semiempirical) mass model as a function of neutron number (top section). Isotopes are connected by lines. The large

80 Years of the liquid drop—50 years of the macroscopic–microscopic model

P. Möller , A.J. Sierk

International Journal of Mass Spectrometry, Volumes 349–350, 2013, 19 - 25

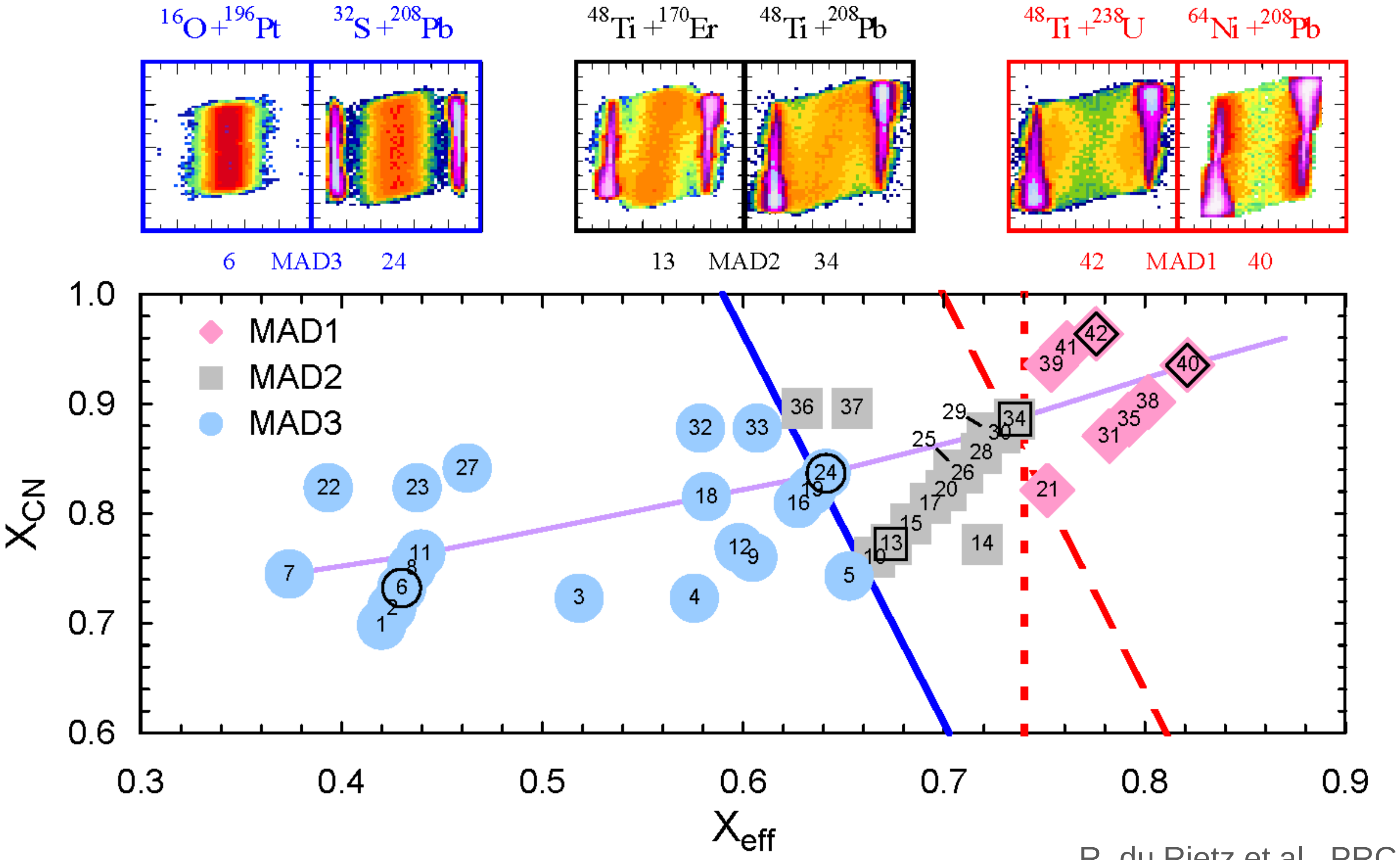

R. du Rietz et al., PRC **88** (2013) 054618

$$x_{\mathrm{CN}} = \frac{(Z^2/A)}{(Z^2/A)_{\mathrm{crit}}} \qquad (Z^2/A)_{\mathrm{crit}} = 50.883\,(1 - 1.7826\,I^2)$$

$$I = (A - 2Z)/A$$

$$x_{\mathrm{eff}} = \frac{4Z_1Z_2/\left[A_1^{1/3}A_2^{1/3}\left(A_1^{1/3} + A_2^{1/3}\right)\right]}{(Z^2/A)_{\mathrm{crit}}}$$

W. J. Swiatecki, Phys. Scr. **24, 113 (1981)**

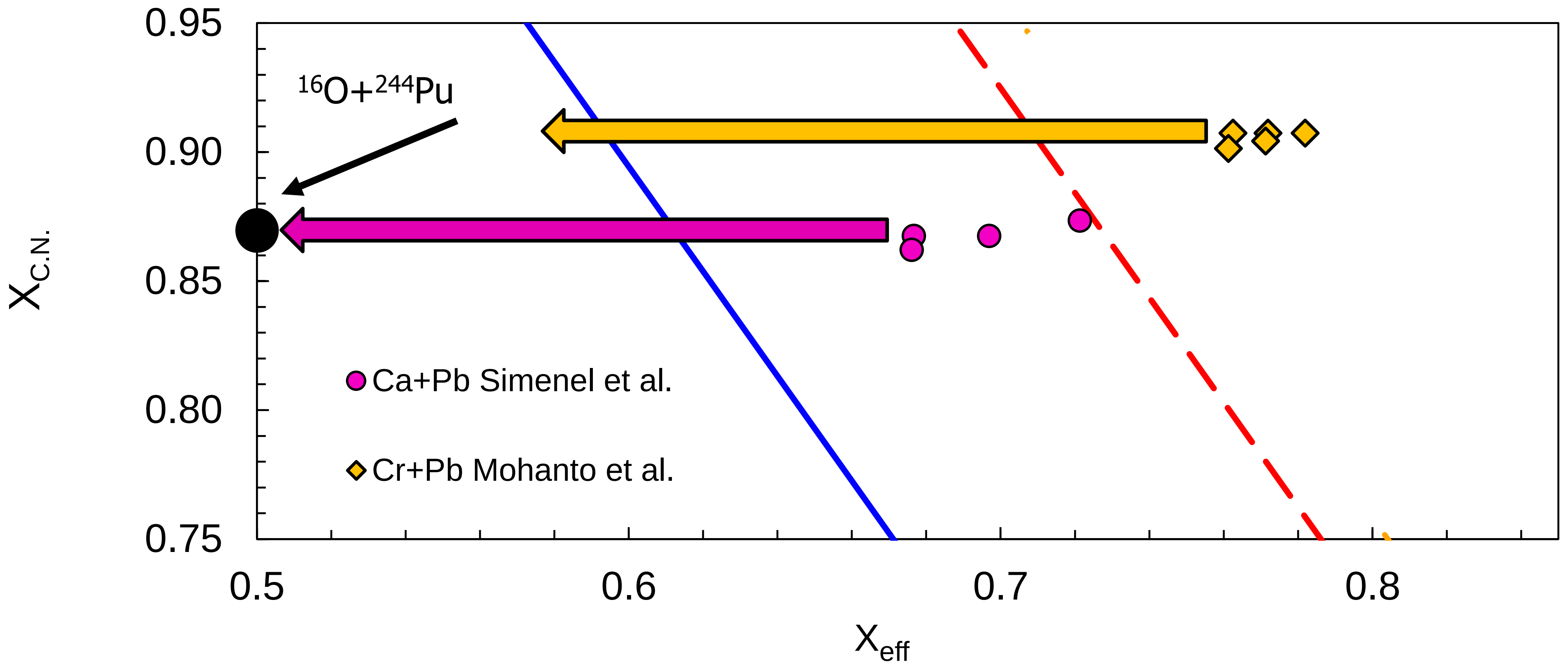

Nuclear structure of the projectile and target can play a very significant role

C. Simenel et al., PLB **710** (2012) 607

G. Mohanto et al., ANU, in preparation

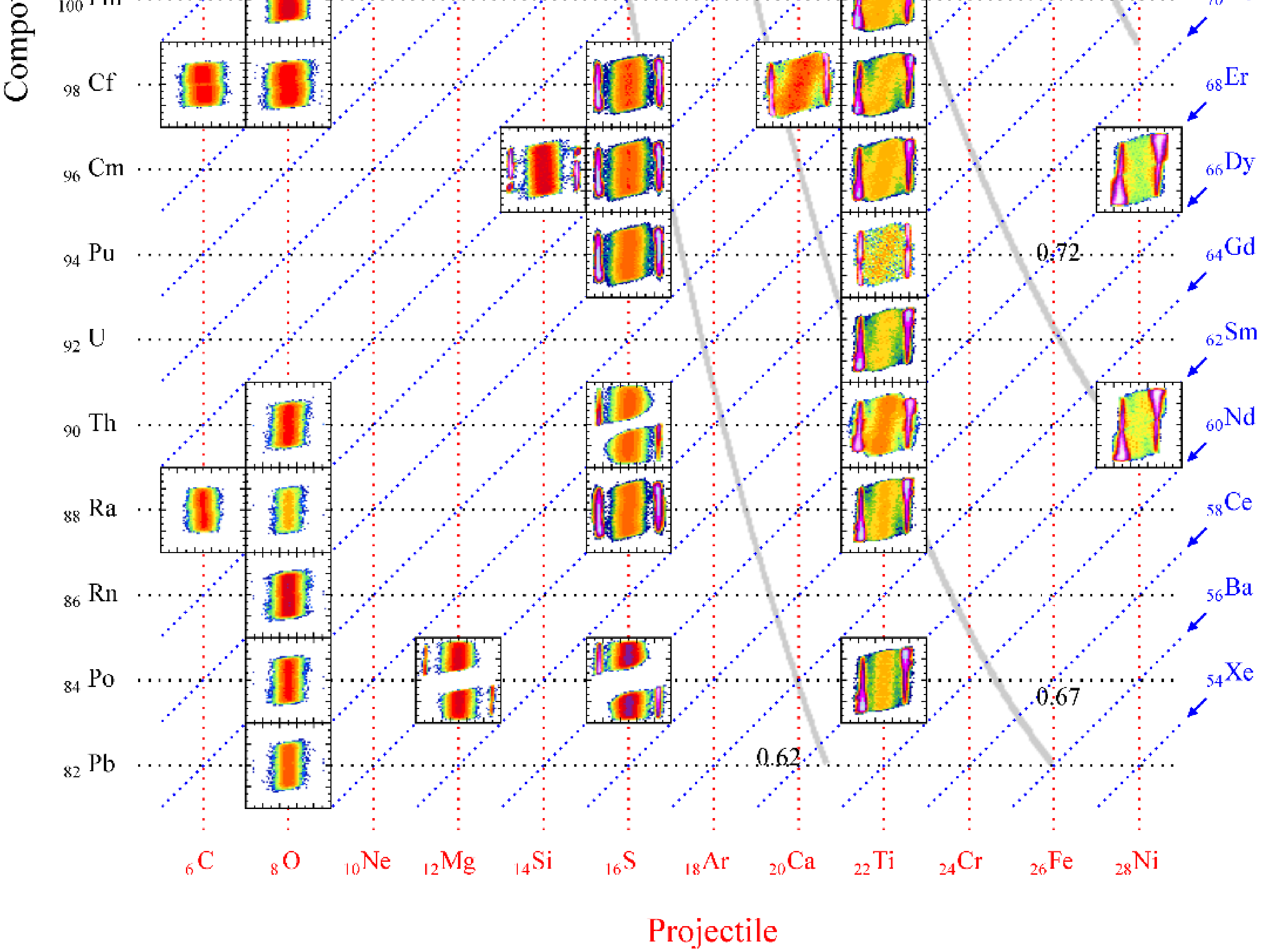

Compo
100 Fm
98 Cf
96 Cm
94 Pu
92 U
90 Th
88 Ra
86 Rn
84 Po
82 Pb
68 Er
66 Dy
64 Gd
62 Sm
60 Nd
58 Ce
56 Ba
54 Xe
0.72
0.67
0.62
6 C
8 O
10 Ne
12 Mg
14 Si
16 S
18 Ar
20 Ca
22 Ti
24 Cr
26 Fe
28 Ni
Projectile

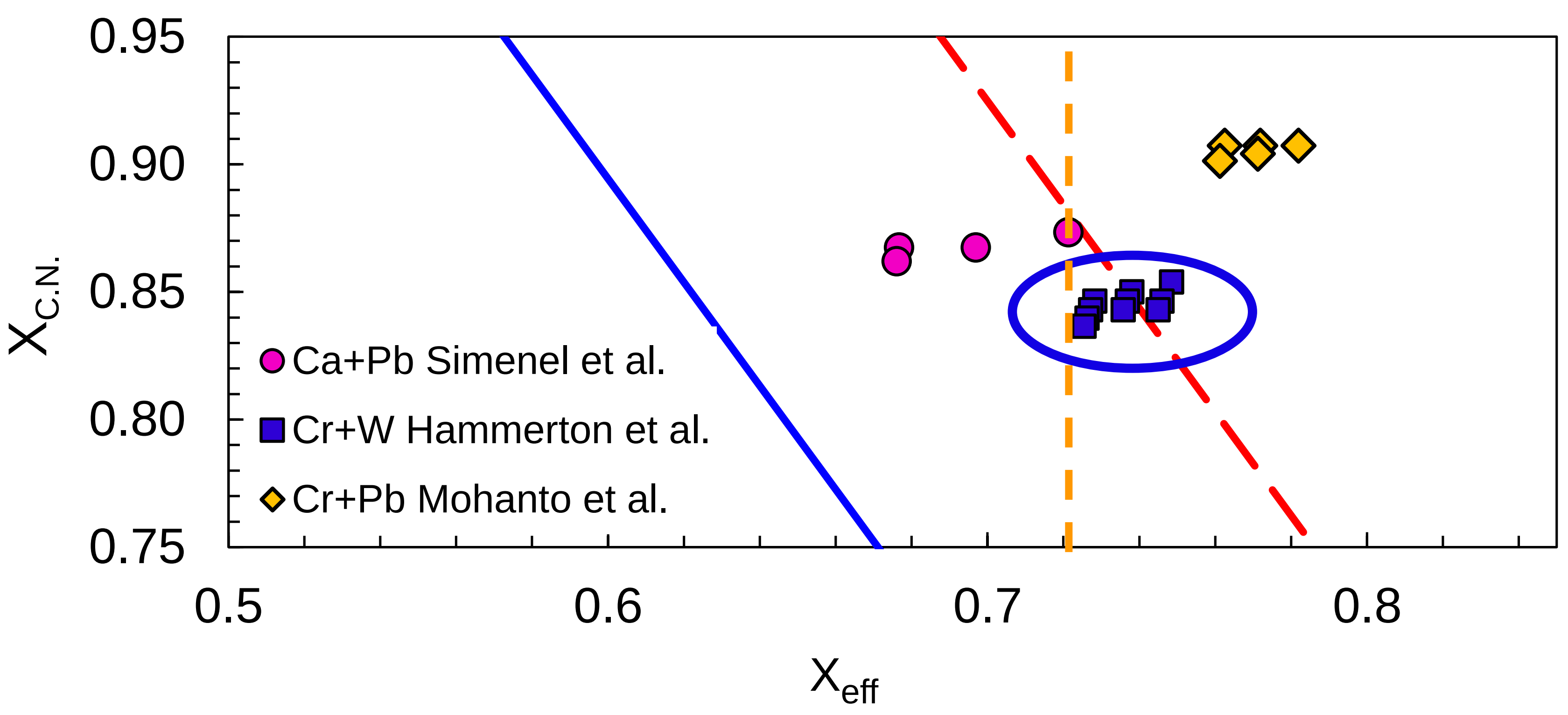

C. Simenel et al., PLB **710** (2012) 607

K. Hammerton et al., PRC **91** (2015) 041602

G. Mohanto et al., ANU, in preparation

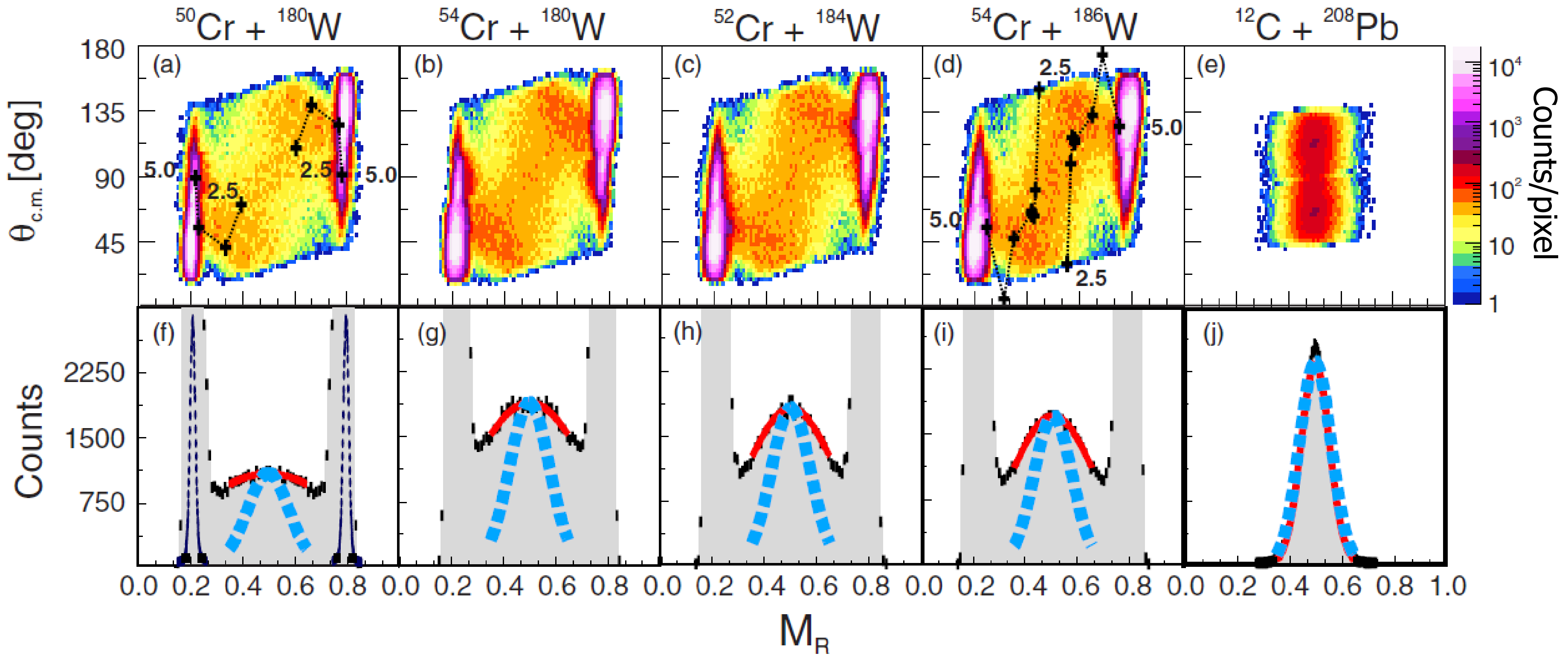

$E/V_B = 1.13$

Smooth change in mass width with neutron number

K. Hammerton et al., PRC **91** (2015) 041602